Article

Asymmetric Oxidation of Enol Derivatives to #-Alkoxy Carbonyls Using Iminium Salt Catalysts: A Synthetic and Computational Study

Philip C. Bulman Page, Saud M. Almutairi, Yohan Chan, G Richard Stephenson, Yannick Gama, Ross L. Goodyear, Alice Douteau, Steven Mark Allin, and Garth A. Jones

Just Accepted

Asymmetric Oxidation of Enol Derivatives to α-Alkoxy Carbonyls Using Iminium Salt Catalysts: A Synthetic and Computational Study

Philip C. Bulman Page,[a]* Saud M. Almutairi,[a] Yohan Chan,[a] G. Richard Stephenson,[a]* Yannick Gama,[a] Ross L. Goodyear,[a] Alice Douteau,[a] Steven M. Allin,[b] Garth A. Jones,[a]*

[a] School of Chemistry, University of East Anglia, Norwich Research Park, Norwich, Norfolk NR4 7TJ, U.K.

[b] Department of Chemistry and Forensics, Nottingham Trent University, Clifton, Nottingham NG11 8NS, U.K.
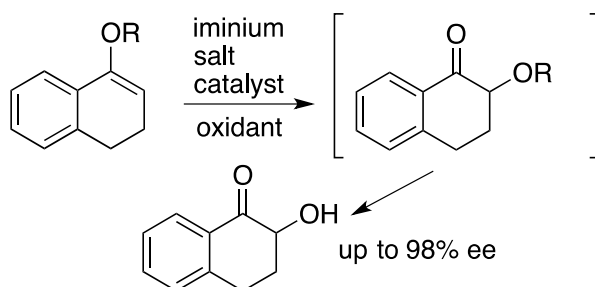
Abstract: We report herein the first examples of asymmetric oxidation of enol ether and ester substrates using iminium salt organocatalysis, affording moderate to excellent enantioselectivities of up to 98% ee for tetralone-derived substrates in the α-hydroxyketone products. A comprehensive density functional theory study was undertaken to interpret the competing diastereoisomeric transition states in this example in order to identify the origins of enantioselectivity. The calculations, performed at the B3LYP/6-31G(D) level of theory, gave good agreement with the experimental results, in terms of the magnitude of the effects under the specified reaction conditions, and in terms of the preferential formation of the (R)-enantiomer. Just one of the 30 characterized transition states dominates the enantioselectivity, which is attributed to the adoption of an orientation relative to stereochemical features of the chiral controlling element that combines a CH–π interaction between a CH_2 group in the substrate and one of the aromatic rings of the biaryl section of the chiral auxiliary with a good alignment of the acetoxy group with the other biaryl ring, and places the smallest substituent on the alkene (a hydrogen atom) in the most sterically-hindered position.

Introduction

The α-hydroxycarbonyl motif is present in many natural products and in intermediates towards their syntheses.[1] A simple method to prepare α-hydroxycarbonyls involves the oxidation of silyl enol ethers, and is known as the Rubottom reaction. Rubottom,[2] Brook,[3] and Hassner[4] first reported the use of *m*-chloroperbenzoic acid to oxidize silyl enol ethers to form α-hydroxy-ketones and aldehydes

in 1974, later followed by the preparation of α-hydroxycarboxylic acids from ketene bis(trimethylsilyl) acetals.[5] Other methodologies include, for example, the oxidation of silyl enol ethers with sulfonyl oxaziridines,[6] osmium tetroxide,[7] hypervalent iodine reagents,[8] aerobic oxidation,[9] and the use of organic-inorganic hybrid polymers as catalysts;[10] and the oxidation of other enol ethers and esters using various organic peracids[11] and dioxiranes.[12]

A number of asymmetric versions have also been developed using chiral oxidants, metal-based catalysts, and organocatalysts,[13] as well as a chiral electrolyte.[14] Davis used chiral sulfonyl oxaziridines to oxidize a range of enolates, and comprehensively reviewed this topic in 1992.[15] Mn(III) (salen) catalysts and various oxidants have been used to obtain α-hydroxycarbonyls in up to 90% ee from silyl enol ethers (Thornton,[17] Adam,[18]), enol ethers and enol acetates (Patonay,[16] Katsuki,[19]). Krawczyk also used Mn(III) (salen) complexes to oxidize enol phosphates in up to 96% ee.[20] Sharpless[21] and Curran[22] reported the asymmetric oxidation of enol ethers using osmium-based catalysts. Yamamoto obtained chiral hydroxyketones from tin enolates[23] and silyl enol ethers[24] using nitrosobenzene and chiral phosphine-silver catalysts in up to 99% ee. Simpkins used chiral bases to obtain chiral hydroxyketones through kinetically controlled deprotonation in up to 74% ee.[25]

Adam,[26] Shi,[27] and Solladié-Cavallo[28] used chiral ketones to catalyse the oxidation of silyl enol ethers in high enantiomeric excesses. Myers more recently used Shi's fructose-derived catalyst in a tandem oxidation-reduction to obtain diols from silyl enol ethers in up to 93% ee.[29]

We have reported catalysts based on dihydroisoquinolinium (e.g. **1**), biphenylazepinium (e.g. **2** and **3**), and binaphthylazepinium (e.g. **4**) units, each of which contains a chiral substituent on the nitrogen atom, for aqueous oxone-driven epoxidation reactions. The most successful of these catalysts contain the (*S,S*)-acetonamine 1,3-dioxane motif (Figure 1).[30]

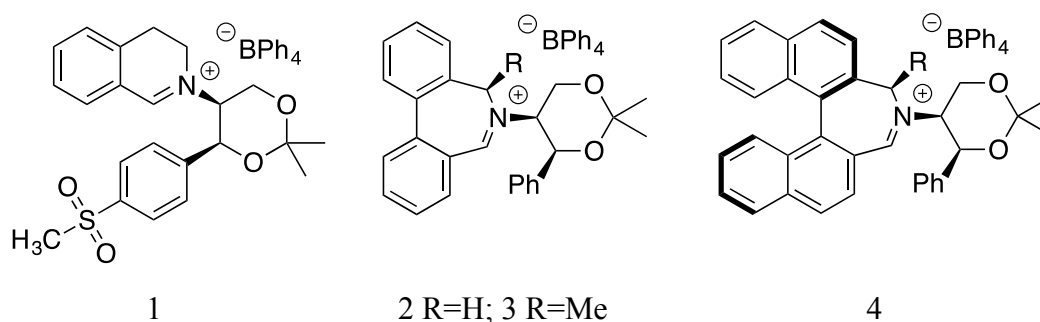**1**   **2** R=H; **3** R=Me   **4**
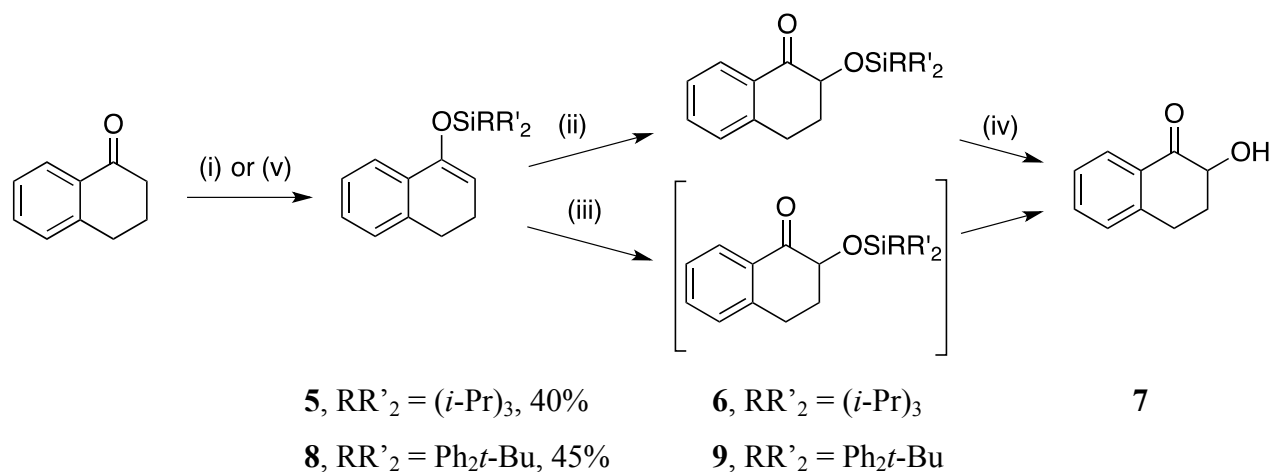
Figure 1: Iminium salt catalysts.

These species provided the first very high enantioselectivities for iminium salt catalysed asymmetric epoxidation of alkenes. We have also developed non-aqueous conditions for the use of these

catalysts, using tetraphenylphosphonium monoperoxysulfate (TPPP)[31] as the oxidant.[32] The asymmetric epoxidation processes utilizing iminium salt catalysts **1** and **2** have been used in syntheses of levcromakalim,[33] (–)-lomatin and (+)-*trans*-khellactone,[34] scuteflorin,[35] and mollugin,[36]. Alternative oxidants such as hydrogen peroxide or sodium hypochlorite,[37] and electrochemically-generated oxidants,[38] may also be used in these iminium salt-catalysed epoxidation reactions.

Herein we report the application of our methodology to the generation of enantiomerically enriched α-hydroxy carbonyls through catalytic asymmetric oxidation of enol derivatives.

Results and discussion

We chose 1-tetralone and its enol derivatives as test substrates. Silyl enol ethers were first investigated; silyl enol ether **5** was prepared using tri-isopropyl silyl triflate and triethylamine as the base.[39] Oxidation of **5** with m-CPBA led to *O*-silyl protected compound **6** In 89% yield. Removal of the silyl group was achieved using one equivalent of camphorsulfonic acid in methanol to yield α-hydroxyketone **7** (Scheme 1). Silyl enol ether **8** was prepared similarly.

5, RR'$_2$ = (*i*-Pr)$_3$, 40%   **6**, RR'$_2$ = (*i*-Pr)$_3$ **7**

8, RR'$_2$ = Ph$_2$*t*-Bu, 45%   **9**, RR'$_2$ = Ph$_2$*t*-Bu

Reagents and conditions: (i): Et$_3$N (2 equiv.), TiPSOTf (1.5 equiv.), CH$_2$Cl$_2$, r.t., 16 h, 40%; (ii): **5**, *m*-CPBA (1.5 equiv.), NaHCO$_3$ (2 equiv.), CH$_2$Cl$_2$, 0 °C to r.t., 16 h, 89% of **6**; (iii): Catalyst (see Figure 1, 0.1 equiv.), TPPP (2 equiv.), CHCl$_3$, 0 °C; (iv): **6**, CSA (1 equiv.), MeOH, r.t., 16 h, 50%; (v): KHMDS (1.8 equiv.), *t*-Bu(Ph)$_2$SiCl (1.4 equiv.), THF, −78°C to r.t., 16 h, 45%.

Scheme 1. Generation and oxidation of silyl enol ethers **5** and **8**

Asymmetric oxidation of **5** and **8** using our catalytic system proceeded smoothly under non-aqueous conditions; a selection of the reaction conditions and results is shown in Table 1. No oxidation by TPPP was observed in the absence of catalyst (entry 1). In some instances using substrate **5**, the silyl group was partially or wholly lost during the reaction/work-up process to give hydroxyketone **7** directly, but in others the intermediate silyloxy species **6** or **9** could be observed. In such cases, hydrolysis to give **7** was readily achieved using camphorsulfonic acid as above, or other hydrolytic

conditions. When the reaction was carried out under aqueous conditions, using Oxone as oxidant, only α-hydroxyketone **7** was obtained after the reaction workup.

Table 1: Optimization of oxidation reaction conditions using substrates **5** and **8**

Entry	Catalyst (10 mol%)	Substrate	Oxidant (2 equiv.)	Temp. /°C	Time /h	Solvent	Conv. /% [a]	Yield /%	ee %[b]	Absolute config. of major enantiomer[c]
1	No cat.	**5**	TPPP	0	24	CHCl$_3$	<5%	-	-	-
2	No cat.	**5**	*m*-CPBA	0	2	CH$_2$Cl$_2$	100	52	-	-
3	**1**	**5**	TPPP	0	12	CHCl$_3$	100	67	20	(−)-(*S*)
4	**1**	**5**	TPPP	−10	12	CHCl$_3$	100	72	24	(−)-(*S*)
5	**1**	**5**	TPPP	−70	24	CHCl$_3$	88	65	43	(−)-(*S*)
6	**2**	**5**	TPPP	0	72	CHCl$_3$	41	32	35	(+)-(*R*)
7	**2**	**5**	TPPP	0	72	CH$_2$Cl$_2$	100	59	13	(+)-(*R*)
8	**2**	**5**	TPPP	0	72	MeCN	100	63	25	(+)-(*R*)
9	**2**	**5**	oxone/ NaHCO$_3$	0	24	MeCN/ H$_2$O	100	89	25	(+)-(*R*)
10	**2**	**8**	TPPP	0	24	CHCl$_3$	91	76	52	(+)-(*R*)
11	**4**	**8**	TPPP	0	24	CHCl$_3$	95	78	50	(+)-(*R*)

(a): Conversions were calculated from ^{1}H NMR spectra of reaction mixtures after work-up for compounds **6**, **7**, and **9**.

(b): Enantioselectivities were measured by CSP HPLC (Daicel Chiralcel OD-H or Knauer Eurocel 01 using isopropanol/hexane as eluent).

(c): The absolute configuration of the major enantiomer was attributed using optical rotation according to the literature.[20]

With TIPS-protected substrate **5**, moderate enantioselectivities were observed: using catalyst **1** in chloroform, the reaction was almost complete after 24 h at −70 °C, giving (−)-(*S*)-α-hydroxyketone **7** in 65% yield (entry 5) (over the two steps) and 43% ee. The reaction proceeds more rapidly but less selectively at higher temperatures (entries 3, 4). Using biphenyl catalyst **2** in chloroform, the enantioselectivity was higher and in the opposite sense (entry 6), but the reaction proceeded more slowly, precluding the use of low temperatures. As previously observed in our studies of epoxidation, chloroform was found to be the solvent which gave the highest level of ee: indeed, changing the solvent improved the conversion at the expense of the selectivity.

Altering the size and shape of the silyl group to *tert*-butyldiphenylsilyl provided a small improvement in enantioselectivity. Using catalyst **2** with TBDPS enol ether **8** at 0 °C provided α-silyloxyketone **9** with 91% conversion (entry 10), from which (+)-(*R*)-α-hydroxyketone **7** was obtained in 52% ee (cf 35% ee from enol ether **5**). Similar results were observed with binaphthyl catalyst **4**, which provided **9** with 95% conversion and (+)-(*R*)-**7** in 50% ee (entry 11).

Given the moderate enantioselectivity observed using silyl enol ethers as substrates, we turned our attention to the oxidation of enol phosphates.[20] α-Tetralone was converted into the corresponding enol phosphate **10** in 69% yield using diethyl phosphorochloridate and LDA as the base, which was submitted to our non-aqueous epoxidation reaction conditions (Scheme 2, Table 2).[40]

10 **7**
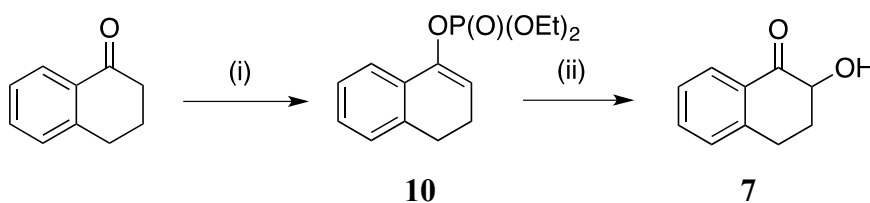
Reagents and conditions: (i) LDA (1 equiv.), (EtO)$_2$P(O)Cl (1.5 equiv.), THF, −78 °C to r.t., 1 h, 69%; (ii) Catalyst (0.1 equiv.), TPPP (2 equiv.), CHCl$_3$.

Scheme 2

Table 2. Oxidation of enol phosphate **10**

Entry	Catalyst (10 mol%)	Oxidant (2 equiv.)	Temp. /°C	Time /h	Solvent	Conv. /%[a]	ee /%[b]	Absolute config. of major enantiomer[c]
1	**1**	TPPP	0	48	CHCl$_3$	45	20	(−)-(*S*)
2	**1**	TPPP	−30	48	CHCl$_3$	22	35	(−)-(*S*)
3	**1**	TPPP	−50	72	CHCl$_3$	-	-	-
4	**2**	TPPP	−30	72	CHCl$_3$	45	90	(+)-(*R*)

(a): Conversions were calculated from ^{1}H NMR spectra of reaction mixtures after work-up.

(b): Enantioselectivities were measured by CSP HPLC (Daicel Chiralcel OD-H using isopropanol/hexane as eluent).

(c): The absolute configuration of the major enantiomer was attributed using optical rotation according to the literature.[20]

In these cases, α-hydroxyketone **7** was isolated directly from the oxidation reaction after work-up and purification. Unfortunately, no increase in enantioselectivity over the silyl enol ether substrates was observed when enol phosphate **10** and catalyst **1** were used (entries 1, 2). Furthermore, the rate

of epoxidation of the phosphate was reduced, no conversion being observed at −50 °C (**entry 3**). When catalyst **2** was used at −30 °C, α-hydroxyketone **7** was obtained in 90% ee (entry 4). Again, however, no reaction was observed when the temperature was lowered to −50 C.

We next turned our attention to enol esters, with acetate, benzoate and trifluoroacetate derivatives chosen as suitable substrates. α-Tetralone was first converted into the corresponding enol acetate **11** in 75% yield using isopropenyl acetate under acidic conditions, which was subjected to our non-aqueous oxidation reaction conditions (Scheme 3, Table 3).[41]

11   **7**
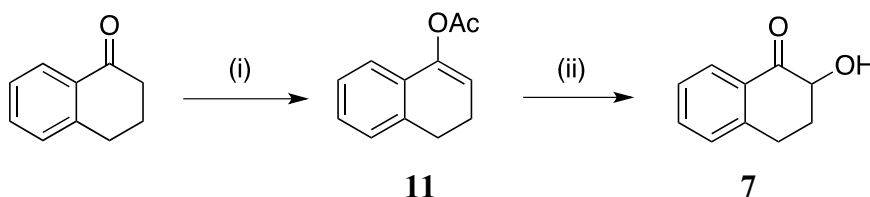
Reagents and conditions: (i) *p*-Toluene sulfonic acid, isopropenyl acetate, reflux, 16 h, 75%; (ii) Catalyst (0.1 equiv.), TPPP (2 equiv.), CHCl$_3$.

Scheme 3

Table 3. Oxidation of enol acetate **11**

Entry	Catalyst (10 mol%)	Temp. /°C	Time /h	Solvent	Conv. /%[a]	ee /%[b]	Absolute config. of major enantiomer[c]
1	**1**	0	24	CHCl$_3$	62	66	(−)-(*S*)
2	**1**	−30	24	CHCl$_3$	42	72	(−)-(*S*)
3	**1**	−30	24	CH$_2$Cl$_2$	62	70	(−)-(*S*)
4	**1**	−30	24	MeCN	70	67	(−)-(*S*)
5	**2**	0	48	CHCl$_3$	99	88	(+)-(*R*)
6	**2**	−30	48	CHCl$_3$	95	97	(+)-(*R*)
7	**2**	−45	48	CHCl$_3$	95	98	(+)-(*R*)
8	**4**	0	48	CHCl$_3$	12	31	(+)-(*R*)
9	**4**	−30	48	CHCl$_3$	5	-	-

(a): Conversions were calculated from ^{1}H NMR spectra of reaction mixtures after work-up.

(b): Enantioselectivities were measured by CSP HPLC (Daicel Chiralcel OD-H using isopropanol/hexane as eluent).

(c): The absolute configuration of the major enantiomer was attributed using optical rotation according to the literature.[20]

Again, α-hydroxyketone **7** was isolated directly from the oxidation reaction after work-up and purification. Although the reaction proceeds more slowly than in the case of the corresponding silyl

enol ethers, the enantioselectivity observed is higher: using catalysts **1** and **2** at 0 ºC, in chloroform, compound **7** was obtained in 66% (entry 1) and 88% ee (entry 5), respectively. Lowering the temperature to –45 ºC led to **7** in 98% ee and 95% conversion when catalyst **2** was used (entry 7).

Initial oxidation results were thus promising, and other enol esters were prepared. 1-Tetralone was converted into the corresponding benzoate and trifluoroacetate enol esters in 26% and 91% yield, respectively, which were oxidized under our standard conditions (Scheme 4, Table 4).

12, R = Bz; **13**, R = COCF$_3$ **7**

Reagents and conditions: (i) (PhCO)$_2$O (1 equiv.), HClO$_4$ (20 mol%), hexanes, r.t., 2 h, 26%; (ii) *p*-Toluene sulfonic acid, (CF$_3$CO)$_2$O, reflux, 16 h, 76%; (iii) Catalyst (0.1 equiv.), TPPP (2 equiv.), CHCl$_3$. 0 °C, 24 h.

Scheme 4

Table 4. Oxidation of enol esters **12** and **13**

Substrate	Catalyst (10 mol%)	Conv. /%[a]	ee /%[b]	Absolute config. of major enantiomer[c]
OBz **12**	**1**	23	65	(−)-(*S*)
	2	35	88	(+)-(*R*)
	4	33	38	(+)-(*R*)
F$_3$C(O)C **13**	**1**	23	54	(−)-(*S*)
	2	65	90	(+)-(*R*)
	4	63	43	(+)-(*R*)

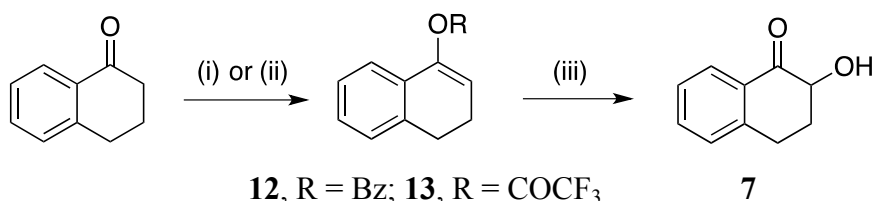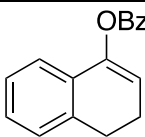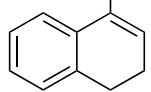(a): Conversions were calculated from ^{1}H NMR spectra of reaction mixtures after work-up.

(b): Enantioselectivities were measured by CSP HPLC (Knauer Eurocel 01 using isopropanol/hexane as eluent).
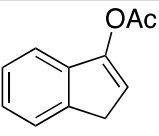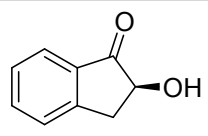
(c): The absolute configuration of the major enantiomer was attributed using optical rotation according to literature data.[20]

Epoxidation of the enol benzoate **12** and enol trifluoroacetate **13** led to the formation of the product **7** in 38-90% ee at 0 °C, similar to the enantioselectivities obtained when the corresponding enol acetate was oxidized. The reactivity of the enol benzoate **12** appears to be lower as conversions were below those observed in the case of **11** over the same time period, perhaps a result of steric hindrance

from the benzoate group. Conversions were higher in the case of the enol trifluoroacetate **13** than the benzoate, despite the presence of the highly electron-withdrawing trifluoro group.

A number of further enol acetates **14** to **17** were subsequently prepared and submitted to our standard epoxidation conditions (Table 5). Enol acetate **16** was prepared from the ketone by a literature route from 3-bromo-N-phenylpropanamide.

Table 5. Oxidation of enol acetates **14 - 17**

Substrate	Yield /%	Product	Temp. /°C	Time /h	Conv. /%[a]	ee /%[b]	Absolute config. of major enantiomer[c]
11	75	**7**	−30	48	95	97	(+)-(*S*)
14	95	**18**	0	24	99	87	(+)-(*S*)
			−30	48	95	92	(+)-(*S*)
15	80	**19**	−30	48	70	78	(−)-(*S*)
16	41	**20**	−30	72	65	67	(−)
17[d]	73	**21**	−30	72	95	59	(−)-(*S*)

Conditions: Catalyst **2** (0.1 equiv.), TPPP (2 equiv.), CHCl$_3$.

(a): Conversions were calculated from ^{1}H NMR spectra of reaction mixtures after work-up.

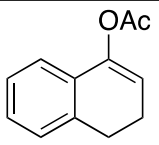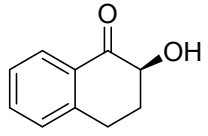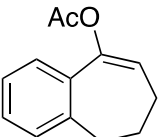(b): Enantioselectivities were measured by CSP HPLC (Knauer Eurocel 01 using isopropanol/hexane as eluent).
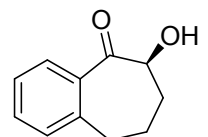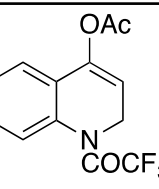
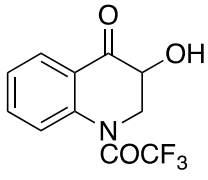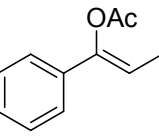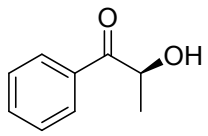(c): The absolute configurations of the major enantiomers were attributed using optical rotations according to literature data.

(d): The *Z* double bond stereochemistry was established by comparison of NMR data with literature values.

We were pleased to find that the reactions proceeded smoothly, and hydroxyketones were obtained with enantioselectivities ranging from 57% to 93% ee. Racemic materials were obtained by MCPBA oxidation. The methodology was applied to the synthesis of the natural product (−)-tatarinoid A **22**.[42] (−)-Tatarinoid A has previously been prepared using a chiral Weinreb amide,[43] and an irregular Wittig reaction,[43,44] respectively. Our synthesis (Scheme 5) began with the nucleophilic addition of ethylmagnesium bromide to 2,4,5-trimethoxybenzaldehyde **23**, forming alcohol **24** in 93% yield. Oxidation of **24** using MnO_2 afforded ketone **25** in 46% yield. Treatment of **25** with LDA and acetic anhydride led to *O*-acetylation of the lithium enolate to afford enol acetate **26**, a method known to give *Z* stereochemistry, which was converted into racemic **27** using MCPBA.

23   **24**   **25**   **26**   **27**
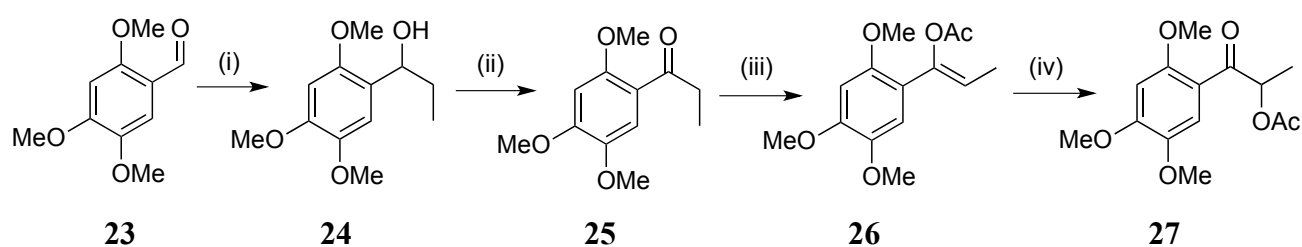
Reagents and conditions: (i): EtMgBr (3M in Et$_2$O, 2 equiv.), THF, 0 °C to rt, 16 h, 93%; (ii): MnO_2 (10 equiv.), CH_2Cl_2, reflux, 24 h, 46%; (iii): DIPA (1.2 equiv.), n-BuLi (1.6 M in hexane, 1.2 equiv.), THF, −78 °C, then Ac$_2$O (2 equiv.), −78 °C to rt, 36 h, 51%; (iv) NaHCO$_3$ (3 equiv.), m-CPBA (1.5 equiv.), CH_2Cl_2, 0 °C to rt, 16 h, 29% over 2 steps.

Scheme 5. Synthesis of the tatarinoid A precursor

Asymmetric oxidation of **26** at −45 °C using TPPP and catalyst **2** took place to give α-acetoxyketone **27** with a moderate enantioselectivity of 50% ee, though in a very low yield of 6%. A 32% yield could be obtained, with an enantioselectivity of 37% ee, using freshly repurified starting material. Deacetylation of **27** (Scheme 6) produced from our most enantioselective result furnished Tatarinoid A in 63% yield with no significant change in ee (48% ee). Optical rotation measurements indicated that the major enantiomer of our non-racemic mixture of tatarinoid A was the naturally occurring (*R*)-(−)-enantiomer.[42]

26   **27**   (*R*)-(−)-Tatarinoid A **22**
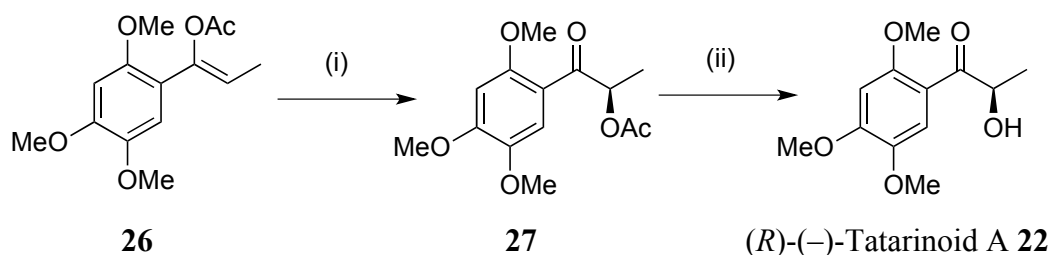
(i) Catalyst **2** (0.1 equiv.), TPPP (2 equiv.), CHCl$_3$; (ii) CSA, MeOH

Scheme 6. Synthesis of (*R*)-(−)-tatarinoid A

Computational study of the transition states

The chiral iminium ion employed in this study is well suited to computational evaluation. It contains two principal chiral features (Figure 2): (1) the axial chirality of the biphenyl unit which in this case is contained in section C7a-C11a-C11b-C4a of the dibenzo[c,e]azepin-6-ium seven-membered ring, and (2) the 4'-phenyl-1',3'-dioxane which is attached at C5' to the nitrogen atom of the azepinium moiety. This dioxane has two stereogenic centres (C4' and C5'). In this examination of asymmetric oxidation of enol ether and ester substrates, iminium ion **2** was used in the 4'*S*,5'*S* configuration (see Figure 1). The C4' phenyl substituent is important for two reasons. First, it desymmetrizes the otherwise symmetrical 5'-substituted 2',2'-dimethyl-1',3'-dioxane ring. Secondly, in combination with the C2' methyl groups, it serves as a conformational lock since the axial orientation of the Ph group would be highly disfavoured (see red box, Figure 2) by the 1,3-diaxial interaction between with the axial methyl group (with two methyl groups at C2', one must always be axial). Given these structures are highly energetically unfavourable, they were excluded from the computational analysis. This considerably simplified the task of assessing the relevant conformations of the iminium ion, and of the derived oxaziridinium ions, in preparation for our study of the transition states for the epoxidation reaction.
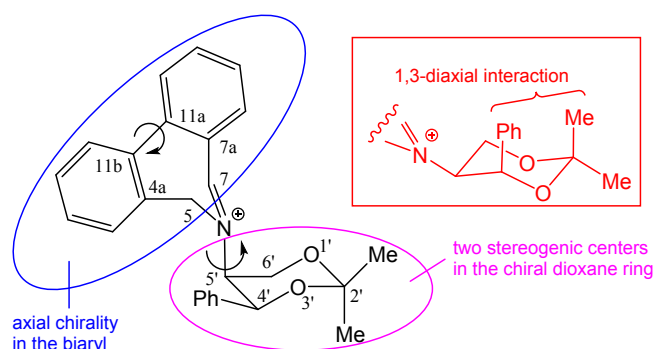
Figure 2. Axial and carbon-centered chirality in the iminium ion **2** (box: potential for a 1,3 diaxial interaction in an alternative chair conformation).

In iminium ion **2**, the two key features of conformational mobility are the possibilities of atropisomeric epimerisation within the dibenzo[c,e]azepin-6-ium ring by variation of the dihedral angle C10a-C11a-C11b-C1 and movement around the C-N bond that connects the azepinium ring to C5' of the dioxane, i.e. variation of the dihedral angle C7-N-C5'-C6'. These two possibilities were examined first in a gas phase DFT study employing the widely used and computationally rapid Becke B3LYP functional[45] with Pople's 6-31G(D)[46] basis set. Four distinct structures for **2** were identified (Table 6, entries 1-4) and were characterised by comparing the 7a-11a-11b-4a (−42.2 - 40.3°) and 7-N-5'-4' (−105.5 - 84.8°) dihedral angles. All four conformations of the iminium ion **2** are within 16 kJ mol⁻¹, and therefore must be considered as potentially important contributors to the

epoxidation mechanism for oxygen atom transfer from the oxaziridinium ion to the alkene.

Table 6. Energies and selected dihedral angles for the four conformations of the iminium ion **2** at optimized geometries.[a]

Entry / Structure	Numbering for the iminium ion	7a-11a-11b-4a	7-N-5'-4'	4a-5-N-5'	N-5'-4'-1"	5'-4'-1"-2"	5'-6'-1'-2'
	Relative Energy (kJ mole^{-1})	(°)	(°)	(°)	(°)	(°)	(°)
1	0.00	40.3	84.8	−111.6	49.5	80.1	53.8
2	4.20	−39.7	−99.1	141.0	46.1	74.8	53.5
3	6.56	−42.2	34.1	113.1	51.0	59.8	59.9
4	15.2	39.3	−100.4	−118.8	47.4	71.5	52.9

[a] the absence of imaginary (negative) vibrational frequencies determined by frequency calculations using the atomic coordinates of the optimised geometries confirmed that in each case true energy minima had been identified.

Table 7. Energies and selected dihedral angles for the four conformations of the oxaziridinium ions **30a**,**d**,**e**,**g**[a] and **30b**,**c**,**f**,**h**[b] at optimized geometries.[c]

Entry / Structure	Numbering for the oxaziridinium ion	4a-11b-11a-7a	4-4a-4b-O	4b-N-5'-4'	7a-7-N-5'	N-5'-4'-1"	5'-4'-1"-2"	5'-6'-1'-2'
	Relative Energy (kJ mole^{-1})	(°)	(°)	(°)	(°)	(°)	(°)	(°)
1 **30a**	0.00[d]	−40.7	152.5	−94.3	137.3	48.0	72.7	53.4
2 **30b**	7.09[e]	41.1	−153.8	74.8	−139.5	50.0	75.5	55.3
3 **30c**	14.97[f]	41.1	−151.9	−156.4	−147.0	50.1	53.6	56.8
4 **30d**	17.85[g]	−41.1	153.3	104.0	146.7	50.9	74.1	55.9
5 **30e**	21.00[e]	41.7	71.8	106.8	−79.6	50.4	75.9	56.8
6 **30f**	30.46[g]	−41.1	−72.6	6.5	82.9	56.1	47.6	52.6
7 **30g**	35.44[f]	39.3	74.8	−94.8	−98.5	49.4	62.8	54.2
8 **30h**	36.76[d]	−40.5	−71.2	−133.7	91.8	45.9	77.6	52.1

[a] positive value for the dihedral angle 4-4a-4b-O; [b] negative value for the dihedral angle 4-4a-4b-O; [c] the absence of imaginary (negative) vibrational frequencies determined by frequency calculations using the atomic coordinates of the optimised geometries confirmed that in each case true energy minima had been identified; [d] conformation corresponds to that of the iminium ion in Table 6, entry 2; [e] conformation corresponds to that of the iminium ion in Table 6, entry 1; [f] conformation corresponds to that of the iminium ion in Table 6, entry 4; [g]: conformation corresponds to that of the iminium ion in entry 3.

The reactive oxaziridinium ions, which were generated *in situ* in the epoxidation process, were evaluated next, at the same level of theory. In the absence of experimental data to guide the choice of diastereoisomers, each iminium ion provided two possible oxaziridinium ions which differed by whether the oxygen was added to the front or rear diastereoface of the C=N double bond (see Figure 3). The energies and key geometric features for the optimized geometries of all eight resulting structures (**30a-h**) are presented in entries 1-8 of Table 7. The range of energies for these eight oxaziridinium ions was broader than in the case of the iminium ions, but was still <40 kJ mole^{-1}. As expected, the central dihedral angle of the biaryl section of these structures was relatively consistent throughout (39.3 - 41.7° or −39.7 - −42.2°), as was C5'-C6'-C1'-C2' (52.1 - 59.9°) which was chosen to illustrate the consistency of the chair character of the 1',3'-dioxane six-membered ring. The dihedral angle C4-C4a-C4b-O (oxaziridinium ion numbering) conveniently indicates the orientation of the additional oxygen atom of the oxaziridinium ion relative to the azepinium ring. Values of about 70° (or –70°) and 150° (or –150°) in the optimised structures show that there is considerable variation in the stereochemical environment of the oxygen (the positive and negative angles reflect the fact that the oxygen is either pointing forwards or pointing backwards). Since this oxygen occupies a position directly beside the point of rotational motion between the two halves of the chiral auxiliary (see Figure 3B and 3C), it is to be expected that its position will significantly influence the conformational preferences about the N-C5' bond. The broader range of dihedral angles at this position (6.5 - 106.8° and –94.3 - –156.4°) observed in the optimised structures of the oxaziridinium ions compared to those of the iminium ions further supports the view that a wide selection of stereochemical environments are present. This will have important consequences for the direction of the approach of the alkene in the competing pathways for the transition states of the epoxidation reaction. Similarly, the C4' phenyl substituent takes up a position close to the oxygen atom in some of the structures and although it reliably occupies an equatorial position [see the narrow range of values for N-C5'-C4'-C1" (45.9 – 56.1°)]. The tilt of the plane of the benzene ring relative to the equatorial plane of the chair six-membered ring shows much more variation and, for example, the C5'-C4'-C1"-C2" dihedral angles range from about 50 to 80°. Interestingly, this variation is present both the iminium ion and oxaziridinium ion series (Figure 3).
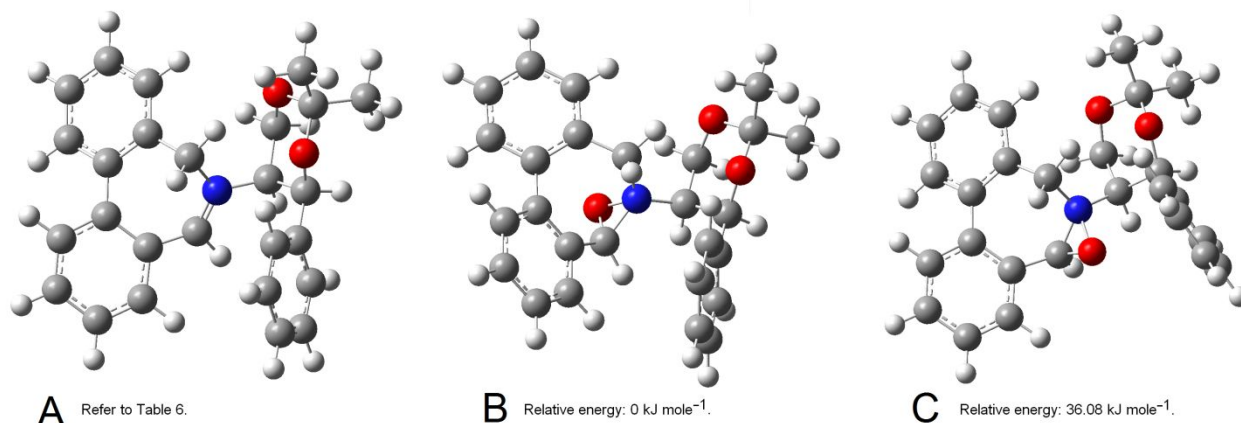
Figure 3. Optimised geometries [B3LYP/ 6-31G(D)] of the most stable conformation of the iminium ion **2** (A) and two derived oxaziridinium ions (B: C4-C4a-C4b-O = 152.5°; C: C4-C4a-C4b-O = −71.2°), **30a**, with the oxygen behind atom (B) and **30h** in front (C) of the dibenzo[c,e]azepin-6-ium ring system.

With the set of eight oxaziridinium ion structures (**30a-h**) now calculated, the influence of the steric effects of the biaryl and phenyl aromatic rings, and the conformation of the molecule about the central N-C5' bond, on the energies of transition states for transfer of O from the oxygen donor (the oxaziridinium ion) to the oxygen acceptor (the alkene), and the relative orientations between the alkene and the C-N-O three-membered ring were now assessed. The extreme possibilities for this latter conformational issue are 'bow-tie'[47] ('butterfly') structures in which all five atoms (the C-N-O ring and the C=C) lie roughly in the same plane (i.e. a central angle of ~180°), and the alternative spiro conformer[48,49] in which the angle between the two planes is about 90°. The latter have already been identified for the enantioselective epoxidation of 1,2-dihydronaphthalene by an oxaziridinium ion.[50] In order to compare our system directly with that of Houk's in his classic computational study[49] of the epoxidation of ethene (using a simpler oxygen donor), all eight transition states for transfers of oxygen from **30a-h** to ethene were calculated. The through-space dihedral angles N-C7-C3'''-C4''' and N-C7-C4'''-C3''' were used to assess whether the transition states were of the 'bow-tie' or 'spiro' types. Despite the variety of steric environments about the C-N-O three-membered ring, it is clear from the data presented in Table 8 that all eight transition states (TSs) for the epoxidation of our model alkene ethene were spiro-like (the magnitudes of the dihedral angles range from 82 to 109°). Each transition state was confirmed by the presence of a negative vibrational frequency, with the reaction coordinate corresponding to the concerted lengthening of the N-O bond upon the approach of the alkene. The reaction paths were confirmed by computing points along each reaction pathway by determining the intrinsic reaction coordinates[51] (IRCs) in both directions.

Table 8. Energies and key geometric features of the transition states for the epoxidation of ethene by **2**.

Level of theory:	B3LYP / 6-31G(D)								TS
Entry	Oxaziridinium ion	Relative TS energies (kJ mole^{-1})	N-O	O-C4'''	N-O-3''	O-C3'''-C4'''	N-C5'-C4'-C1''	N-C7-C3'''-C4'''	N-C7-C3'''-C4'''	
			(Å)	(Å)	(°)	(°)	(°)	(°)	(°)	
1	**30a**[a]	0.00	1.89	2.12	159.4	75.0	47.3	−91.8	102.4	spiro
2	**30b**[b]	3.41	1.87	2.19	160.1	72.5	48.5	−98.5	95.7	spiro[b]
3	**30c**[c]	14.70	1.87	2.17	158.9	72.0	52.7	−100.2	93.3	spiro[c]
4	**30d**[d]	19.95	1.83	2.21	157.7	74.8	52.6	−94.6	98.7	spiro
5	**30e**[e]	30.46	1.89	2.15	158.7	72.1	50.4	−82.1	108.3	spiro[e]
6	**30f**[f]	33.87	1.87	2.12	160.1	76.5	48.1	−100.4	89.5	spiro
7	**30h**[g]	39.91	1.91	2.12	159.9	75.3	50.6	−108.5	82.1	spiro
8	**30g**[h]	41.48	1.91	2.11	160.3	72.7	46.6	−87.3	103.0	spiro[h]

a: see Table 7, entry 1; b: see Table 7, entry 2; c: see Table 7, entry 3; d: see Table 7, entry 4; e: see Table 7, entry 5; f: see Table 7, entry 6; g: see Table 7, entry 8; h: see Table 7, entry 7.

The highest enantioselectivity (98% ee) in the experimental survey of epoxidation reactions described above (Table 3) was achieved by the epoxidation of the enol acetate **11** using iminium salt **2** and TPPP to generate the oxaziridinium ions. In order to extend the computational study to unsymmetrical prochiral substrates such as **11**, analogous transition states to those in Table 7 were calculated using enol acetate as the oxygen atom acceptor (see Figure 4).
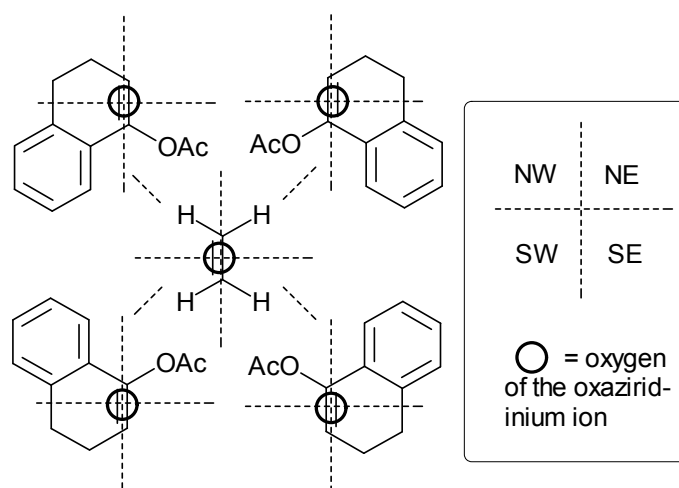
Figure 4. Four different orientations of the enol acetate **11** relative to the chiral features (not drawn)

of each of the proposed oxaziridinium ions **30a-h** in which the acetoxy substituent lies in the SE, SW, NW or NE quadrants, respectively, working clockwise from the top-left structure (box: key to the quadrants relative to the central ethene TS, and the representation of the oxaziridinium ion lying below the alkene).

The transition state calculations were again performed using the B3LYP/ 6-31G(D) level of theory, but with solvent effects (chloroform) taken into account by employing the polarizable continuum model,[52] and with a temperature of 233.15 K (−45° C). Of the 32 possible transition states that could in principle contribute to the enantioselectivity, thirty were located. In the remaining two possibilities, the enol acetate ring system clashes with structural features of the oxaziridinium ion. While there was room for ethene to approach the oxygen atom, the larger enol acetate structure **11**, was sterically hindered. Consequently, these two transition states were removed from the analysis under the assumption that they would be so high in energy, as not to contribute to the population statistics.

The results are presented in Table 9 and indicate that the oxygen transfer process is dominated by just one of the transition state structures (entry 1). This corresponds to the oxaziridinium ion **30a**, which was also responsible for the most significant transition state identified for the epoxidation of ethene (Table 7, entry 1). The oxaziridinium ions relating to the top four entries in Table 9 (**30a** and **30b**) are derived from two most stable iminium ion conformations (Table 6, entries 1 and 2). In this respect, the outcomes of the transition state calculations for ethene and the enol acetate **11** are similar, but there are also significant differences. Because of the interactions between the prochiral alkene and the chiral features of the oxaziridinium ion, almost all the transition states are displaced away from the expected spiro form, taking on twisted conformations intermediate between spiro and bow-tie. Indeed, three of the TSs were sufficiently flat around the central oxygen atom to be regarded as bow-tie. Neither of the two spiro TSs (entries 14, 22) and none of the bow-tie TSs (entries 17, 19 and 30) contribute significantly to the *R/S* selectivity. It is the distortion of the spiro conformation into the twisted structures that provides evidence for the presence of strong controlling interactions that underlie the enantioselectivity of the reaction. The results obtained for **11** also reveal a significant mechanistic difference. Analysis of the reaction pathways for each transition state by the intrinsic reaction coordinate method shows that the oxygen transfer process no longer directly forms the epoxide products, but instead, in almost all cases, a cationic intermediate was identified at the end of each pathway. An example corresponding to Table 9, entry 1 is presented in Figure 5B. The presence of the aromatic ring in **11** would be expected to stabilise positive charge α to the ring (i.e. at C4''') and so displace the transfer of the oxygen atom to C3'''. Although not so strongly electron-donating as an ether substituent, the OAc group, which is also present at C4''', can similarly be

expected to contribute to the stabilisation of the developing C4''' cation in the transition states.

Table 9. Energies and conformations of the transition states for the epoxidation of 4-acetoxy-1,2-dihydronaphthalene **11**.

Level of theory:		B3LYP/6-31G(D); solvent[a] = CHCl₃; temp. = 233.15 K (−45 °C)								TS
Entry	Oxazirid- inium ion	Relative TS energies (kJ mole^{-1})	Config. of product	N-O	O-C3'''	O-C3'''-C4'''	N-O- C3'''-C4'''	N-C7-C3'''-C4'''	N-C7-C4'''-C3'''	
				(Å)	(Å)	(°)	(°)	(°)	(°)	
1	**30a**[b]	0.00[c]	R	1.75	2.31	100.8	128.1	−136.8	52.5	twisted[d]
2	**30a**[b]	6.95[e]	S	1.77	2.35	88.7	−176.6	−80.0	107.3	twisted
3	**30b**[f]	7.46[g]	S	1.74	2.34	100.7	−124.4	134.4	−55.7	twisted
4	**30a**[b]	8.81[h]	R	1.75	2.34	92.2	61.0	115.6	−78.3	twisted
5	**30c**[i]	10.34	R	1.76	2.35	91.6	123.1	−58.2	−139.1	twisted
6	**30b**[f]	11.46	R	1.77	2.29	102.6	125.2	−136.5	52.9	twisted
7	**30b**[f]	12.83[j]	S	1.77	2.34	99.7	−43.8	−142.8	46.0	twisted
8	**30b**[f]	12.83[h,k]	R	1.74	2.42	87.7	171.2	76.6	−114.0	twisted
9	**30c**[i]	12.83[l]	S	1.75	2.31	102.4	120.0	140.9	−48.9	twisted
10	**30c**[i]	17.14	S	1.77	2.29	93.7	−49.7	−140.3	48.9	twisted
11	**30c**[i]	17.15	R	1.74	2.31	101.3	94.6	−159.4	26.4	twisted
12	**30d**[m]	26.50	S	1.75	2.34	101.9	−108.4	150.1	−38.0	twisted
13	**30d**[m]	27.12	S	1.76	2.40	94.9	−130.4	83.8	−102.3	twisted
14	**30d**[m]	31.55	S	1.77	2.38	95.1	148.4	−91.1	98.7	spiro[n]
15	**30d**[m]	33.27	R	1.79	2.40	94.5	−156.5	107.5	−82.1	twisted
16	**30g**[o]	35.10	S	1.78	2.33	89.2	179.7	59.2	−125.5	twisted
17	**30g**[o]	35.35	R	1.85	2.25	107.6	117.0	173.0	−8.4	bow-tie[p]
18	**30e**[q]	37.28	S	1.79	2.35	99.3	164.1	70.0	−115.6	twisted
19	**30e**[q]	38.20	R	1.83	2.27	106.8	169.0	−171.7	10.1	bow-tie
20	**30f**[f]	38.60	S	1.81	2.27	103.4	−152.3	166.9	−15.6	twisted
21	**30f**[f]	39.12	R	1.77	2.33	93.8	168.4	−108.4	79.7	twisted
22	**30f**[f]	40.20	R	1.76	2.34	93.5	−175.9	−95.3	91.6	spiro
23	**30f**[f]	42.25	R	1.82	2.29	101.3	132.7	138.1	−47.6	twisted
24	**30g**[o]	42.44	S	1.81	2.27	101.8	−174.2	−153.3	30.7	twisted
25	**30g**[o]	42.76[s]	R	1.77	2.41	82.1	123.5	−45.5	138.1	twisted

26	**30h**[t]	43.12	S	1.86	2.25	110.8	−106.1	−116.6	16.4	twisted
27	**30e**[q]	45.69[s]	R	1.80	2.34	88.6	128.6	−61.0	124.8	twisted
28	**30h**[t]	48.87	R	1.77	2.33	95.5	173.0	−62.1	123.5	twisted
29	**30h**[t]	50.64	R	1.83	2.31	100.6	166.5	129.2	−57.6	twisted
30	**30h**[t]	76.27	S	1.78	2.36	92.4	−176.4	1.0	−179.1	bow-tie

a: using the polarizable continuum model as implemented by Gaussian 09; b: see Table 7, entry 1; c: Boltzman population: 0.811; d: (magnitude of dihedral ~11-89 or 99-171); e: Boltzman population: 0.06; f: see Table 7, entry 2; g: Boltzman population: 0.03; h: taken from a single point calculation using the coordinates from a transition state characterised in the gas phase at 233.15 K; i: see Table 7, entry 3; j: 12.831 kJ mole^{-1}; k: 12.832 kJ mole^{-1}; l: 12.833 kJ mole^{-1}; m: see Table 7, entry 4; n: (magnitude of dihedral ~ 90); o: see Table 7, entry 7; p: (magnitude of dihedral ~180) bow-tie; q: see Table 7, entry 5; r: see Table 7, entry 6; s: path goes directly to the epoxide (no cationic intermediate was identified); t: see Table 7, entry 8.
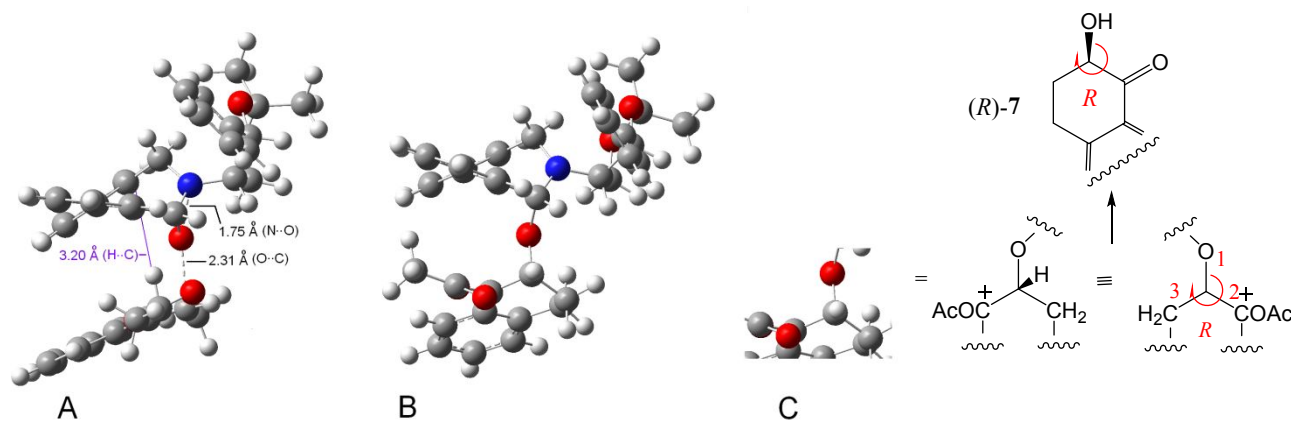

Figure 5. A: The twisted transition state (derived from the approach of the enol acetate **11** to the oxaziridinium ion **30a** with the acetoxy group in the NE quadrant) which dominates the enantioselectivity. B: Oxygen transfer to **11** initially forms a cationic intermediate. C: The induced stereogenic center of the structure shown in B is redrawn to illustrate its conversion into (*R*)-**7**. The calculations were performed at the B3LYP/6-31G(D) level of theory.

The transition state enthalpies from Table 9 were corrected with zero-point energies and Gibbs free energies. These thermodynamically corrected energies were then used to calculate Boltzmann populations at 233.15 K, for each of the transition states. In these calculations we assume that all eight reactant oxaziridinium ion conformations interconvert under the reaction conditions, and hence the contribution of all of the transition states to the overall enantioselectivity was then calculated, resulting in a predicted ee of 81% in favour of the (*R*)-enantiomer. This is in qualitative agreement with the experimental value of 98% ee. The data presented here is sufficient to establish which one of the 30 characterised transition states is primarily responsible for the control of enantioselectivity, and so provide a sound basis to explore in future work the structural issues that account for the exceptionally high efficiency of the epoxidation reaction presented in Table 3.
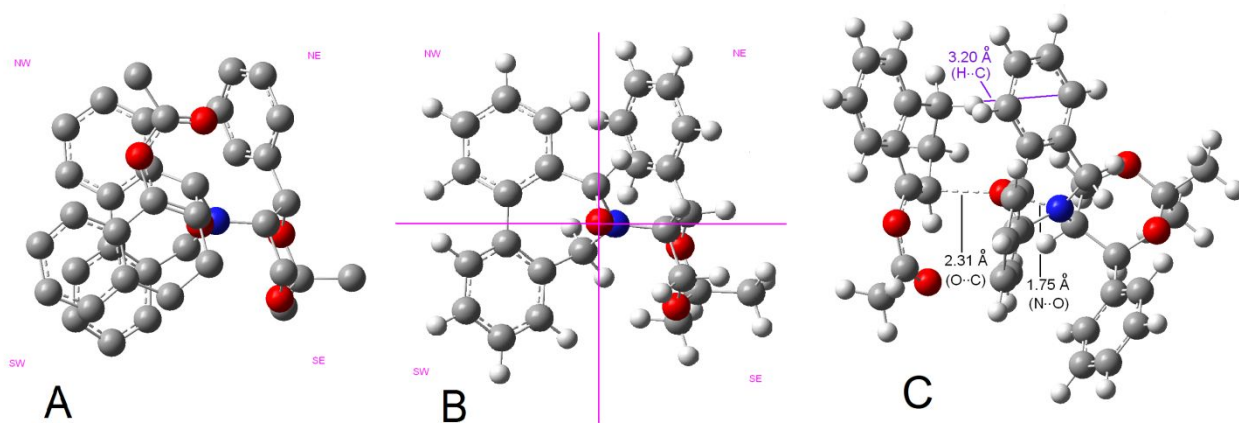
Figure 6. A: The dominant transition state (shown in Figure 5A) viewed from the top looking down on the 4-acetoxy-1,2-dihydronaphthalene substrate (hydrogen atoms removed for clarity). B: As in A, but with the hydrogen atoms shown and the substrate removed to reveal the oxaziridinium ion **11** more clearly (quadrants labelled as in Figure 4). C: Side view showing the close approach of one of the methylene hydrogen atoms at C1''' in the 4'''-acetoxy-1''',2'''-dihydronaphthalene to the C4 position in one of the aromatic rings in the biphenyl section of **11** (H··C4 distance: 3.20 Å), and the overlap of the acetoxy substituent with the second arene in **11**. The calculations were performed at the B3LYP/6-31G(D) level of theory.

Inspection of the conformation of the dominant transition state (Figure 6; see also Figure 5A and Table 9, entry 1) shows that the acetoxy group of the 1,2-dihydronaphthalene occupies in the NW quadrant, and the arene of the 1,2-dihydronaphthalene occupies the SW quadrant, which allows the C3''' C-H substituent of the C3'''=C4''' double bond to be directed towards the NE and SE quadrants which are partially blocked by the phenyl substituent (NE) and the 2',2'-dimethyl-1',3'-dioxane ring of the oxaziridinium ion (SE). This is the orientation of the 1,2-dihydronaphthalene that suffers the least from steric interactions, so allowing the alkene to come close to the oxygen of the lowest energy oxaziridinium ion (the C··O distance is 2.31 Å). The NW quadrant is occupied by one of the arenes of the biaryl section of the oxaziridinium ion, but this is oriented so that its π-system is side-on, raising the possibility of a favourable association with the carbonyl group of the acetoxy substituent (closest O··C distance, 3.45 Å). Figure 6A also shows, in the SW quadrant, the overlap of aromatic rings of the substrate and the chiral auxiliary (closest C··C distance, 3.99 Å), when viewed from the top. These π-system interactions may provide supplementary positive stabilising effects but the main steric contribution to enantioselectivity is the adoption of an orientation relative to stereochemical features of the chiral auxiliary that orientates the smallest substituent on the alkene (a hydrogen atom) towards the most hindered quadrants. NCI calculations were performed to compare through-space non-covalent interactions in the lowest energy (*R*)-selective and the lowest two (*S*)-selective transition states (Entries 1, 2 and 3, respectively, in Table 9).[53] This identified the presence

of CH–π interactions[54] (Figure 7) which bring the one of the hydrogens of the CH$_2$ group at C1''' of the 4'''-acetoxy-1''',2'''-dihydronaphthalene close to the six carbons (C1, C2, C3, C4, C4a, C11b) of the biaryl section of the iminium ion to form a stabilizing interaction. Additional details are provided in the Supporting Information.
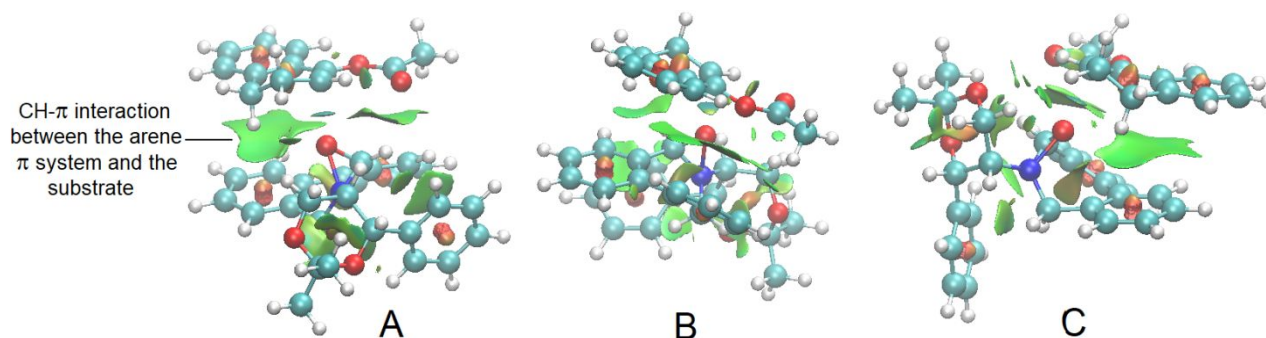

Figure 7. Non-covalent interactions (pale green surfaces) in the three most accessible competing transition states for the oxygen transfer step of the epoxidation of the enol acetate **11** calculated at the B3LYP/6-31G(D) level of theory (solvent: CHCl$_3$; temperature: 233.15 K). A: (*R*)-selective transition state (Table 9, entry 1); B: (*S*)-selective transition state (Table 9, entry 2); C: (*S*)-selective transition state (Table 9, entry 3).

CH–π interactions can contribute as much as 4 kJ mole^{-1} to the energy difference that accounts for enantioselectivity.[55] Figure 7B (viewing the iminium ion in the same orientation as in Figure 7A) shows that this CH–π interaction is more off-centre than in Figure 7A (see Supporting Information). The third lowest energy transition state, (Table 9, entry 3), like its lowest energy counterpart, also has a well-formed CH–π interaction but has a noticeably less extensive interaction surface between the acetoxy group of the substrate and the second aromatic ring of the biaryl section of the oxaziridinium ion. On this basis, it seems probable that the presence of the CH–π interactions shown in Figure 7 make a substantial contribution to the conformational restrictions that control the oxygen transfer process, with the steric effects discussed above accounting for the differences between them, and ultimately the (*R*)-selectivity of epoxidation. Further synthetic work to develop a new generation of biphenylazepinium-based chiral auxiliaries to improve enantioselectivity for the other enol acetate, trifluorocetate and benzoate substrates shown in Tables 4 and 5, and the synthetically valuable example **26**, can now be based on strategies that retain the CH–π interaction and employ it as a pivot point to determine the nature of stereocontrolling steric interactions with other features introduced into the chiral auxiliary.

Conclusions

Oxaziridinium ions generated *in situ* from the chiral iminium salt (4'*S*,5'*S*)-**2** by oxidation with TPPP

are efficient oxygen donors for the epoxidation of alkenes, particularly the 4-acetoxy-1,2-dihydronaphthalene **11**, which, after hydrolysis, affords the (*R*)-hydroxyketone product **12** in 98% ee. The most stable of the eight possible oxariridinium ions plays by far the most significant role in the control of enantioselctivity in this reaction, adopting an orientation relative to stereochemical features of the chiral auxiliary that places the smallest substituent on the alkene (a hydrogen atom) in the more hindered quadrants. In the more accessible transition states, the substrate and the oxaziridinium unit are brought together by CH–π interactions between a CH_2 group in the substrate and one of the aromatic rings of the biaryl section of the chiral auxiliary. The combination of CH–π interactions with the avoidance of adverse steric clashes between the substrate and the chiral auxiliary explains why this most accessible transitions states so strongly dominate the induction of asymmetry in the oxygen-transfer process. The chiral iminium ions used in this study are effective in promoting the epoxidation of a range of enol esters and other alkenes, often providing products in high ee. The reaction has been successfully employed in the synthesis of the natural product tatarinoid A.

Experimental Detail

General procedure for the synthesis of enol acetates [56]

The ketone (approx. 20 mmol), isopropenyl acetate (100 mL) and *p*-toluenesulfonic acid monohydrate (0.1 equiv) were heated using a heating mantle in a Dean-Stark apparatus overnight. The mixture was poured into saturated aqueous $NaHCO_3$ (50 mL) and diethyl ether (100 mL). The organic phase was separated and the aqueous layer extracted with diethyl ether (3 × 100 mL). The combined ethereal solutions were washed with saturated aqueous $NaHCO_3$, saturated aqueous NaCl, dried over anhydrous $MgSO_4$, filtered, and the solvents removed under reduced pressure. The enol acetate was isolated by column chromatography on silica gel (eluent: hexanes/ethyl acetate 5:1).

3,4-Dihydronaphth-1-yl acetate 11 [57]

Prepared according to the general procedure for the synthesis of enol acetates using 1-tetralone (2.5 g, 17 mmol), isopropenyl acetate (100 mL) and *p*-toluenesulfonic acid monohydrate (0.3 g, 0.1 equiv., 1.7 mmol) to give the desired product as a colourless oil (2.4 g, 75%). ν_{max} (film)/cm^{-1} 3100, 2900, 1740, 1650, 1570, 1200; ^{1}H NMR (400 MHz, CDCl₃) δ 7.21 – 7.10 (m, 4H), 5.73 (t, *J* = 4.7 Hz, 1H), 2.89 (t, *J* = 8.1 Hz, 2H), 2.53 – 2.43 (m, 2H), 2.32 (s, 3H); ^{13}C{^{1}H} NMR (100 MHz, CDCl₃) δ 169.2, 145.6, 136.3, 130.1, 128.6, 127.8, 126.2, 120.4, 115.1, 26.9, 23.4, 20.3.

6,7-Dihydro-5H-benzo[7]annulen-9-yl acetate 14 [58]

Prepared according to the general procedure for the synthesis of enol acetates using 1-benzosuberone (2.5 g, 15 mmol), isopropenyl acetate (100 mL) and *p*-toluenesulfonic acid monohydrate (0.26 g, 0.1

equiv., 1.5 mmol) to give the desired product as a colourless oil (3.0 g, 95%). v_{max} (film) /cm^{-1}: 2930, 2858, 1755; ^{1}H NMR (500 MHz, CDCl$_3$) δ 7.42 (d, J = 6.3 Hz, 1H), 7.32 – 7.25 (m, 3H), 5.91 (t, J = 6.2 Hz, 1H), 2.92 (t, J = 1.7 Hz, 2H), 2.24 (s, 3H), 2.23 – 2.19 (m, 2H), 2.16 – 2.10 (m, 2H); ^{13}C{^{1}H} NMR (126 MHz, CDCl$_3$) δ 169.6, 146.0, 141.9, 134.6, 129.2, 128.2, 126.1, 125.5, 119.7, 33.8, 31.3, 25.4, 20.9.

1H-Inden-3-yl acetate 15 [59]

Prepared according to the general procedure for the synthesis of enol acetates using 1-indanone (2.5 g, 19 mmol), isopropenyl acetate (100 mL) and *p*-toluenesulfonic acid monohydrate (0.3 g, 0.1 equiv., 1.9 mmol) to give the desired product as a yellow oil (2.66 g, 80%). v_{max} (film)/cm^{-1}: 2991, 1700, 1450, 1200; ^{1}H NMR (500 MHz, CDCl$_3$) δ 7.51 (d, J = 6.5 Hz, 1H), 7.44 – 7.30 (m, 3H), 6.42 (t, J = 2.3 Hz, 1H), 3.47 (d, J = 2.4 Hz, 2H), 2.39 (s, 3H); ^{13}C{^{1}H} NMR (126 MHz, CDCl$_3$) δ 168.2, 149.1, 141.8, 139.1, 126.3, 125.7, 124.1, 118.1, 115.5, 35.0, 21.1.

1-Phenylprop-1-enyl acetate 17 [60]

Prepared according to the general procedure for the synthesis of enol acetates using propiophenone (2.5 g, 18 mmol), isopropenyl acetate (100 mL) and *p*-toluenesulfonic acid monohydrate (0.3 g, 0.1 equiv., 1.8 mmol) to give the desired product, a yellow oil, as a 10:1 mixture of *Z:E* isomers (2.4 g, 73%). v_{max} (film) /cm^{-1}: 3000, 1696, 1500. For the major isomer: ^{1}H NMR (500 MHz, CDCl$_3$) δ 7.45 – 7.31 (m, 5H), 7.31 – 7.29 (m, 0.5H), 5.93 (q, J = 7.0 Hz, 1H), 5.57 (q, J = 7.4 Hz, 0.1H), 2.34 (s,3H), 2.18 (s, 0.3H), 1.85 (d, J = 7.4 Hz, 0.3H), 1.75 (d, J = 7.0 Hz, 3H); ^{13}C{^{1}H} NMR (126 MHz, CDCl$_3$) δ 168.6, 146.9, 146.2, 128.4, 128.0, 124.2, 112.6, 20.6, 11.5.

3,4-Dihydronaphthalen-1-yl 2,2,2-trifluoroacetate 13

A mixture of 1-tetralone (1:0 g, 6.8 mmol) and trifluoroacetic anhydride (50 mL) was heated overnight and poured into saturated aqueous NaHCO$_3$ (50 mL) and diethyl ether (100 mL). The organic phase was separated, and the aqueous layer extracted with diethyl ether (3 × 100 mL). The combined ethereal solutions were washed with aqueous saturated NaHCO$_3$, saturated aqueous NaCl, dried over anhydrous MgSO$_4$, filtered, and the solvents removed under reduced pressure. The corresponding enol trifluoroacetate was isolated by column chromatography on silica gel (eluent: hexanes/ethyl acetate 5:1) to give the desired product as a yellow oil (1.5 g, 91%). v_{max} (film) /cm^{-1}; 2944, 2838, 1700; ^{1}H NMR (500 MHz, CDCl$_3$) δ 7.29 – 7.20 (m, 3H), 7.13 (d, J = 6.7 Hz, 1H), 5.96 (t, J = 4.7 Hz, 1H), 2.93 (t, J = 8.2 Hz, 2H), 2.57 – 2.50 (m, 2H); ^{13}C{^{1}H} NMR (126 MHz, CDCl$_3$) δ 144.8, 136.3, 128.7, 128.6, 127.8, 126.7, 120.3, 116.3, 114.6 (q, CF$_3$, J = 289 Hz), 30.9, 27.1, 21.9.

1-(2,2,2-Trifluoroacetyl)-1,2-dihydroquinolin-4-yl acetate 16

Following the general procedure for the synthesis of enol acetates using 1-(2,2,2-trifluoroacetyl)-2,3-dihydroquinolin-4(1H)-one[61] (2.5 g, 10 mmol), isopropenyl acetate (100 mL) and *p*-toluenesulfonic acid monohydrate (0.2 g, 0.1 equiv., 1.1 mmol) to give the desired product as yellow oil (1.2 g, 41%). ν_{max} (film) /cm^{-1}; 3000, 1755, 1702, 1600, 1484, 1269, 1209; ^{1}H NMR (500 MHz, CDCl$_3$) δ 8.05 (dd, J = 7.9, 1.6 Hz, 1H), 7.73 (dd, J = 8.5, 1.9 Hz, 1H), 7.63 – 7.56 (m, 1H), 7.39 – 7.32 (m, 1H), 5.44 (dd, J = 9.6, 4.4 Hz, 1H), 4.35 (dd, J = 13.7, 4.4 Hz, 1H), 4.14 (dd, J = 13.8, 9.6 Hz, 1H), 2.13 (s, 3H). ^{13}C{^{1}H} NMR (126 MHz, CDCl$_3$) δ 188.2, 169.3, 141.4, 135.1, 128.5, 127.4, 125.1, 124.1, 117.3, 116.2 (q, CF$_3$, J = 288 Hz), 70.7, 48.9, 20.4. HMRS (APCI-FTMS) *m/z*: [M+H]$^+$ calcd for [C$_{13}$H$_{10}$F$_3$NO$_3$+H] 286.0686; Found 286.0685.

(3,4-Dihydronaphthalen-1-yl)oxy)triisopropylsilane 5

The ketone (1.45 g, 5 mmol) and triethylamine (2.09 ml, 9.0 mmol) were dissolved in dichloromethane (15 ml). Triisopropylsilyl triflate (4 ml, 6.0 mmol) was added and the reaction mixture stirred overnight. The ethereal solution was concentrated under reduced pressure and the residue purified by column chromatography on basic alumina using hexane as the eluent to give the enol ether as yellow oil (1.20 g, 40%), ν_{max} (film) /cm^{-1}: 2943, 2860, 1640, 1256; ^{1}H NMR (400 MHz, CDCl$_3$) δ 7.57 (d, J = 6.3 Hz, 1H), 7.25 – 7.11 (m, 3H), 5.19 (t, J = 4.7 Hz, 1H), 2.82 – 2.73 (t, J = 8.2 Hz, 2H), 2.37 – 2.27 (m, 2H), 1.36 – 1.26 (m, 3H), 1.16 (d, J = 7.2 Hz, 18H); ^{13}C{^{1}H} NMR (101 MHz, CDCl$_3$) δ 148.4, 137.1, 133.7, 127.1, 126.8, 126.1, 121.9, 103.8, 28.2, 22.2, 18.1, 12.8.

3,4-Dihydronaphthalen-1-yl diethylphosphonate 10 [62]

Diisopropylamine (2.94 ml, 21 mmol) was dissolved in anhydrous THF (50 ml) and the solution cooled to –78 °C. *n*-BuLi (8.4 ml, 21 mmol, 2.5 M in hexane) was added dropwise. α-Tetralone (2.68 g, 20 mmol) was dissolved in anhydrous THF (10 ml) at –78 °C and the LDA solution was added. The mixture was stirred under an argon atmosphere for 1 h at –78 °C. Diethylphosphorochloridate (5.1 g, 30 mmol) was dissolved in anhydrous THF (5 ml), and the solution added dropwise to the reaction mixture. The mixture was allowed to reach room temperature and stirred for 1 h. The solvents were removed under reduce pressure, the residue was dissolved in diethyl ether (100 mL), and the solution washed with saturated NH$_4$Cl (50 mL) and water (50 mL). The organic layer was dried over anhydrous MgSO$_4$, filtered, and the solvents removed under reduced pressure. The residue was purified using silica gel column chromatography using petroleum ether-EtOAc (5:1 v/v) as the eluent to give the enol phosphate as a yellow oil (2.93 g, 69%). ν_{max} (film) /cm^{-1}: 3000, 1240, 1600; ^{1}H NMR (400 MHz, CDCl$_3$) δ 7.45 (d, J = 6.2 Hz, 1H), 7.25 – 7.13 (m, 3H), 5.91 (t, J = 4.7 Hz, 1H), 4.28 – 4.19 (m, 4H), 2.83 (t, J = 8.1 Hz, 2H), 2.47 – 2.40 (m, 2H), 1.38 (t, J = 7.1 Hz, 6H); ^{13}C{^{1}H} NMR (100 MHz, CDCl$_3$): δ 145.4, 137.0, 131.2, 128.3, 127.6, 126.8, 121.9, 111.5, 67.0, 65.9, 26.2, 22.1, 16.8.

3,4-Dihydronaphthalen-1-yl benzoate 12 [39]

1-Tetralone (2.5 g, 17 mmol) and benzoic anhydride (3.8 g, 16 mmol) were dissolved in hexane (100 mL), and perchloric acid (0.2 mL) added. The mixture was stirred at room temperature for 2 h, and filtered to remove the solids formed. The filtrate was washed with NaOH (1N, 100 mL), saturated $NaHCO_3$ (100 mL), and brine (100 mL), dried over anhydrous Na_2SO_4, filtered, and concentrated under reduced pressure. The residue was purified using silica gel column chromatography using n-pentane/ethyllactate (6:2) to afford 3,4-dihydronaphthalen-1-yl benzoate as a colourless liquid (1.09 g, 26%). v_{max} (film) /cm^{-1}: 3000, 2841, 1736, 1500; ^{1}H NMR (500 MHz, CDCl$_3$) δ 8.25 (dd, J = 8.2, 1.1 Hz, 2H), 7.71 – 7.65 (m, 1H), 7.56 (t, J = 7.7 Hz, 2H), 7.24 – 7.15 (m, 4H), 5.88 (t, J = 4.7 Hz, 1H), 2.97 (t, J = 8.1 Hz, 2H), 2.59 – 2.52 (m, 2H); ^{13}C{^{1}H} NMR (126 MHz, CDCl$_3$) δ 165.0, 145.8, 136.4, 133.5, 130.5, 130.1, 129.5, 128.6, 128.0, 127.6, 126.4, 120.8, 115.7, 27.5, 22.1.

tert-Butyl-[(3, 4-dihydronaphthalen-1-yl)oxy]diphenylsilane 8 [63]

Potassium hexamethyldisilazide (0.7 g, 3.5 mmol) was dissolved in tetrahydrofuran (12 mL), and the solution cooled to −78 °C. Tetralone (0.3 g, 2.0 mmol) was added dropwise by syringe. The resulting pale-brown solution was stirred for 20 min at −78 °C. *tert*-Butylchlorodiphenylsilane (0.75 mL, 2.7 mmol) was added dropwise. The mixture was stirred for 5 min at −78 °C, allowed to reach room temperature, and stirred for 1 h. The solvents were removed under reduced pressure. The pale yellow oily residue was dissolved in pentane (20 mL), the solution was filtered through a pad of celite, and the filtrate was concentrated under reduced pressure. The residue was purified using silica gel column chromatography (hexanes) to provide *tert*-butyl((3,4-dihydronaphthalen-1-yl)oxy)diphenylsilane as a colourless solid (0.35 g, 45%). mp = 64-69 °C [Lit.[63] mp 69 °C]; v_{max} (film) /cm^{-1}: 2937, 2700, 1638, 1250, 1113; ^{1}H NMR (500 MHz, CDCl$_3$) δ 7.72 – 7.69 (m, 4H), 7.35 – 7.02 (m, 10H), 4.69 (t, J = 4.7 Hz, 1H), 2.58 (t, J = 7.9 Hz, 2H), 2.09 – 1.89 (m, 2H), 1.04 (s, 9H); ^{13}C{^{1}H} NMR (126 MHz, CDCl$_3$) δ 145.6, 135.1, 133.3, 131.3, 130.7, 127.6, 125.5, 125.2, 124.9, 124.2, 119.7, 103.6, 25.9, 24.5, 19.9, 17.4.

General Procedure for enol ether/ester oxidation

A. Using MCPBA

$NaHCO_3$ (2 equiv.) was suspended in dichloromethane (2 mL per 100 mg of enol ether/ester) and the mixture cooled to 0 °C. Meta-chloroperoxybenzoic acid (77% w/w; 1.5 equiv.) was added. The mixture was stirred for 10 min. The enol ether/ester (0.2 g) was added, and the reaction followed by TLC until complete consumption of the starting material was observed. Diethyl ether was added (10 mL) and the mixture washed with water (10 mL), aqueous Na_2CO_3 (3 x 10 mL), and brine (10 mL). The organic phase was dried over anhydrous Na_2SO_4, and the solvents removed under reduced

pressure. The residue was purified using column chromatography on silica gel (eluent: hexanes/ethyl acetate 95:5) to give the desired compound.

B. Using TPPP

The catalyst (0.1 equiv.) and the enol ether/ester were dissolved in chloroform/acetonitrile/dichloromethane (2 mL per 100 mg of enol ether/ester), and the mixture was cooled. TPPP (2 equiv.) was added, and the reaction followed by TLC until complete consumption of the starting material was observed. Diethyl ether was added (10 mL) and the reaction mixture was filtered on a pad of celite. The solvents were removed under reduced pressure and the residue purified using column chromatography on silica gel (eluent: hexanes/ethyl acetate 95:5) to give the desired compound.

2-[(Triisopropylsilyl)oxy]-3,4-dihydronaphthalen-1(2H)-one 6

Prepared according to the general procedure for enol ether/ester oxidation using ((3,4-dihydronaphthalen-1-yl)oxy)triisopropylsilane **5** (0.20 g, 0.73 mmol), meta-chloroperoxybenzoic acid (0.17 g) and sodium bicarbonate (0.10 g, 1.11 mmol) to give 2-((triisopropylsilyl)oxy)-3,4-dihydronaphthalen-1(2H)-one (0.19 g, 89%). v_{max} (film) /cm^{-1}: 2941, 2865, 1700, 1903, 1295. ^{1}H NMR: δH (500 MHz; CDCl$_3$): 7.96 (d, J = 7.8 Hz, 1H), 7.39 (t, J = 7.4 Hz, 1H), 7.18 (dd, J = 16.4, 8.9 Hz, 2H), 4.41 (dd, J = 10.3, 4.4 Hz, 1H), 3.13 − 2.86 (m, 2H), 2.32 − 2.09 (m, 2H), 1.18 − 1.05 (m, 3H), 1.03 (d, J = 5.8 Hz, 18H). ^{13}C{^{1}H} NMR (126 MHz, CDCl$_3$) δ 197.2, 143.5, 133.3, 132.0, 128.6, 127.7, 126.5, 74.7, 32.9, 27.1, 17.9, 12.2.

1-Oxo-2,3-dihydro-1H-inden-2-yl acetate [64]

Prepared according to the general procedure for enol ether/ester oxidation using 1H-inden-3-yl acetate **15** (0.50 g, 2.8 mmol), meta-chloroperoxybenzoic acid (1.40 g) and sodium bicarbonate (0.40 g, 4.7 mmol) to give 1-oxo-2,3-dihydro-1H-inden-2-yl acetate (0.25 g, 46%). v_{max} (film) /cm^{-1}: 2932, 1745, 1726. ^{1}H NMR (500 MHz, CDCl$_3$) δ 7.82 (d, J = 7.7 Hz, 1H), 7.67 (td, J = 7.6, 1.1 Hz, 1H), 7.50 − 7.41 (m, 2H), 5.45 (dd, J = 8.0, 4.9 Hz, 1H), 3.68 (dd, J = 16.9, 8.0 Hz, 1H), 3.07 (dd, J = 16.9, 4.8 Hz, 1H), 2.21 (s, 3H). ^{13}C{^{1}H} NMR (126 MHz, CDCl$_3$) δ 200.6, 170.4, 150.4, 135.9, 134.5, 128.1, 126.6, 124.5, 74.0, 33.4, 20.8.

1-Oxo-1-phenylpropan-2-yl acetate [65]

Prepared according to the general procedure for enol ether/ester oxidation using 1-phenylprop-1-en-1-yl acetate **17** (0.2 g, 1.1 mmol), meta-chloroperoxybenzoic acid (0.3 g) and sodium bicarbonate (0.2 g, 2.3 mmol) to give 1-oxo-1-phenylpropan-2-yl acetate (0.1 g, 40%). v_{max} (film) /cm^{-1}: 3004, 1764, 1206. ^{1}H NMR (500 MHz, CDCl$_3$) δ 7.35 − 7.22 (m, 5H), 3.12 (q, J = 5.3 Hz, 1H), 2.07 (s, 3H), 1.40 (d, J = 5.3 Hz, 3H). ^{13}C{^{1}H} NMR (126 MHz, CDCl$_3$) δ 169.1, 136.1, 128.8, 128.5, 125.5,

84.9, 61.3, 21.0, 13.8.

5-Oxo-6,7,8,9-tetrahydro-5H-benzo[7]annulen-6-yl acetate [66]

Prepared according to the general procedure for enol ether/ester oxidation using 6,7-dihydro-5H-benzo[7]annulen-9-yl acetate **14** (1 g, 5 mmol), meta-chloroperoxybenzoic acid (1.2 g) and sodium bicarbonate (0.8 g, 9.5 mmol) to give 5-oxo-6,7,8,9-tetrahydro-5H-benzo[7]annulen-6-yl acetate (0.6 g, 56%). ^{1}H NMR (500 MHz, CDCl$_3$) δ 7.72 – 7.68 (m, 1H), 7.19 (dd, J = 5.7, 3.4 Hz, 2H), 7.02 (dd, J = 5.4, 3.6 Hz, 1H), 3.52 (t, J = 4.7 Hz, 1H), 3.20 – 3.09 (m, 1H), 2.68 – 2.59 (m, 1H), 2.20 – 2.12 (m, 1H), 1.97 (s, 3H), 1.93 – 1.83 (m, 1H), 1.61 – 1.42 (m, 2H).

General procedure for protecting group removal

The substrate was dissolved in methanol (5 mL per 100 mg of starting material) and camphorsulfonic acid (1.1 equiv) added. The reaction was followed by TLC until complete consumption of the starting material was observed. The solvents were removed under reduced pressure and residue purified using column chromatography on silica gel (eluent: hexanes/ethyl acetate 3:1) to give the corresponding α-hydroxy-carbonyl species.

2-Hydroxy-3,4-dihydronaphthalen-1(2H)-one 7 [67]

From 2-((triisopropylsilyl)oxy)-3,4-dihydronaphthalen-1(2H)-one

2-((Triisopropylsilyl)oxy)-3,4-dihydronaphthalen-1(2H)-one **6** (0.2 g, 0.6 mmol) was dissolved in methanol (10 mL), and camphorsulphonic acid (0.16 g, 0.6 mmol) was added. The reaction was followed by TLC until complete consumption of the starting material was observed. The solvents were removed under reduced pressure and the residue was purified using column chromatography on silica gel to give 2-hydroxy-3,4-dihydronaphthalen-1(2H)-one (0.05 g, 50%) ν$_{max}$ (film) /cm^{-1}: 3475, 3066, 1686, 1603. ^{1}H NMR (400 MHz, CDCl$_3$) δ 8.07 (dd, J = 7.8, 1.2 Hz, 1H), 7.55 (td, J = 7.5, 1.4 Hz, 1H), 7.37 (t, J = 7.6 Hz, 1H), 7.30 (d, J = 7.8 Hz, 1H), 4.41 (dd, J = 13.5, 5.4 Hz, 1H), 3.24 – 3.00 (m, 2H), 2.62 – 2.50 (m, 1H), 2.15 – 1.98 (m, 1H). ^{13}C{^{1}H} NMR (100 MHz, CDCl$_3$): δ 199.6, 144.3, 134.2, 130.4, 128.9, 127.6, 126.9., 73.9, 31.9, 27.8.

Asymmetric oxidation

Prepared according to the general procedure for TPPP enol ether/ester epoxidation, catalyst (0.1 equiv) and the enol ether (1 equiv) to give 2-hydroxy-3,4-dihydronaphthalen-1(2H)-one.

For non-racemic material: $[\alpha]_D^{20}$ = +13 (c = 0.03, CHCl$_3$); 88% ee. Literature value:[68] $[\alpha]_D^{20}$ = +11 (c = 0.7, CHCl$_3$); 31% ee.

2-Hydroxy-2,3-dihydro-1H-inden-1-one 19 [69]

Prepared according to the general procedure for protecting group removal using 1-oxo-2,3-dihydro-

1H-inden-2-yl acetate (0.15 g, 0.8 mmol) and camphorsulphonic acid (0.20 g, 0.9 mmol) to give 2-hydroxy-2,3-dihydro-1H-inden-1-one (0.1 g, 86%). ν_{max} (film) /cm^{-1}: 3414, 2923, 1718, 1609. ^{1}H NMR (500 MHz, CDCl$_3$) δ 7.80 (d, J = 7.7 Hz, 1H), 7.67 (td, J = 7.5, 1.2 Hz, 1H), 7.53 – 7.41 (m, 2H), 4.58 (dd, J = 7.9, 5.1 Hz, 1H), 3.62 (dd, J = 16.5, 7.9 Hz, 1H), 3.05 (dd, J = 16.5, 5.1 Hz, 1H). ^{13}C{^{1}H} NMR (126 MHz, CDCl$_3$) δ 206.5, 150.9, 135.9, 134.0, 128.0, 126.8, 124.4, 74.3, 35.1.

For non-racemic material: $[\alpha]_D^{20}$ = –16 (c = 0.04, CHCl$_3$); 78% ee. Literature value:[69] $[\alpha]_D^{20}$ = +54 (c = 1, MeOH); 97% ee.

2-Hydroxy-1-phenylpropan-1-one 21 [70]

Prepared according to the general procedure for protecting group removal using 1-oxo-1-phenylpropan-2-yl acetate (0.10 g, 0.5 mmol) and camphorsulphonic acid (0.10 g, 0.5 mmol) to give 2-hydroxy-1-phenylpropan-1-one (0.07 g, 89%). ν_{max} (film) /cm^{-1}: 3459, 2979, 1682. ^{1}H NMR (500 MHz, CDCl$_3$) δ 7.86 (dd, J = 8.3, 1.1 Hz, 2H), 7.58 – 7.53 (m, 1H), 7.44 (t, J = 7.8 Hz, 2H), 5.15 – 5.04 (m, 1H), 1.38 (d, J = 7.0 Hz, 3H). ^{13}C{^{1}H} NMR (126 MHz, CDCl$_3$) δ 202.4, 134.0, 133.3, 128.8, 128.6, 69.3, 22.3. For non-racemic material: $[\alpha]_D^{20}$ = –25 (c = 0.02, CHCl$_3$); 59% ee. Literature value:[70] $[\alpha]_D^{20}$ = –64.4 (c = 7.8, CHCl$_3$); >98% ee.

6-Hydroxy-6,7,8,9-tetrahydro-5H-benzo[7]annulen-5-one 18 [71]

Prepared according to the general procedure for protecting group removal using 5-oxo-6,7,8,9-tetrahydro-5H-benzo[7]annulen-6-yl acetate (0.10 g, 0.5 mmol) and camphorsulphonic acid (0.10 g, 0.5 mmol) to give 6-hydroxy-6,7,8,9-tetrahydro-5H-benzo[7]annulen-5-one (0.06 g, 75%). ν_{max} (film) /cm^{-1}: 3420, 3055, 2998, 1635. ^{1}H NMR (500 MHz, CDCl$_3$) δ 7.66 (dd, J = 7.7, 1.3 Hz, 1H), 7.34 (td, J = 7.5, 1.5 Hz, 1H), 7.26 – 7.21 (m, 1H), 7.14 (d, J = 7.6 Hz, 1H), 5.36 (dd, J = 10.7, 5.9 Hz, 1H), 3.02 – 2.86 (m, 2H), 2.21 – 2.11 (m, 2H), 2.00 – 1.89 (m, 1H), 1.82 – 1.70 (m, 1H). ^{13}C{^{1}H} NMR (126 MHz, CDCl$_3$) δ 199.6, 170.2, 141.6, 132.0, 130.0, 129.1, 126.8, 34.1, 29.2, 23.5, 20.7. For non-racemic material: $[\alpha]_D^{20}$ = +28 (c = 0.03, CHCl$_3$); 92% ee. Literature value:[71] $[\alpha]_D^{22}$ = +43.4 (c = 0.23, CHCl$_3$); 98% ee.

3-Hydroxy-1-(2,2,2-trifluoroacetyl)-2,3-dihydroquinolin-4(1H)-one 20

NaHCO$_3$ (0.1 g, 1.1 mmol) was suspended in dichloromethane (4 mL), and the mixture cooled to 0 °C. Meta-chloroperoxybenzoic acid (77% w/w; 0.19 g) was added. The mixture was stirred for 10 min. 1-(2,2,2-Trifluoroacetyl)-1,2-dihydroquinolin-4-yl acetate **16** (0.2 g, 0.7 mmol) was added. The reaction was followed by TLC until complete consumption of the starting material was observed. Diethyl ether was added (10 mL) and the mixture was washed with water (10 mL), aqueous Na$_2$CO$_3$ (30 mL), and brine (10 mL). The organic phase was dried over anhydrous Na$_2$SO$_4$ and the solvents removed under reduced pressure. The residue was purified using column chromatography on silica

gel to give 4-oxo-1-(2,2,2-trifluoroacetyl)-1,2,3,4-tetrahydroquinolin-3-yl acetate (0.1 g, 50%).

4-Oxo-1-(2,2,2-trifluoroacetyl)-1,2,3,4-tetrahydroquinolin-3-yl acetate (0.15 g, 0.5 mmol) was dissolved in methanol (5 mL), and camphorsulphonic acid (0.1 g, 0.5 mmol) was added. The reaction was followed by TLC until complete consumption of the starting material was observed. The solvents were removed under reduced pressure, and the residue was purified using column chromatography on silica gel to give 3-hydroxy-1-(2,2,2-trifluoroacetyl)-2,3-dihydroquinolin-4(1H)-one (0.1 g, 78%). ν_{max} (film) /cm^{-1}: 3394, 3000, 1696, 1257. ^{1}H NMR (500 MHz, CDCl$_3$) δ 8.04 (dd, J = 7.8, 1.6 Hz, 1H), 7.85 (d, J = 8.3 Hz, 1H), 7.62 – 7.56 (m, 1H), 7.33 (td, J = 7.9, 1.0 Hz, 1H), 4.45 (dd, J = 12.4, 5.3 Hz, 1H), 3.73 – 3.63 (m, 2H). ^{13}C{^{1}H} NMR (126 MHz, CDCl$_3$) δ 194.8, 142.3, 136.2, 135.2, 128.2, 127.2, 124.2, 123.6, 119.0, 116.2 (q, CF$_3$, J = 288 Hz) 71.5. HRMS (ASAP-TOF) *m/z*: [M+H]$^+$ calcd for [C$_{11}$H$_8$F$_3$NO$_3$+H] 260.0529; Found 260.0535. For non-racemic material: $[\alpha]_D^{20}$ = –33 (c = 0.3, CHCl$_3$); 67% ee.

1-(2,4,5-Trimethoxyphenyl)propan-1-ol 24 [72]

2-(2,4,5-Trimethoxyphenyl)acetaldehyde **23** (5.00 g, 25.48 mmol) was dissolved in anhydrous tetrahydrofuran (135 mL), and the solution cooled to 0 °C. A solution of EtMgBr (17.0 mL, 3 M in Et$_2$O, 50.97 mmol, 2 equiv.) was added slowly. The mixture was stirred at 0 °C for 30 min and allowed to stand for 16 h at room temperature. Saturated aqueous NH$_4$Cl (25 mL) was added and the solvents removed under reduced pressure. Water (50 mL) and diethyl ether (40 mL) were added and the aqueous phase was extracted with Et$_2$O (2 x 40 mL). The combined organic phases were washed with water (60 mL) and brine (60 mL), dried (MgSO$_4$), and the solvents removed under reduced pressure to furnish 1-(2,4,5-trimethoxyphenyl)propan-1-ol as a yellow oil (5.36 g, 93%); mp 71 – 72 °C [lit.[69] 68 – 70 °C]; ν_{max} (CH$_2$Cl$_2$)/cm^{-1} 3494 (broad), 2962, 2935, 2834, 1509, 1464, 1205, 1038; ^{1}H NMR (500 MHz, CDCl$_3$) δ 0.93 (t, J = 7.4 Hz, 3H), 1.68 – 1.83 (m, 2H), 2.43 (br, 1H), 3.81 (s, 3H), 3.83 (s, 3H), 3.87 (s, 3H), 4.77 (dd, J = 7.4, 5.9 Hz, 1H), 6.50 (s, 1H), 6.87 (s, 1H); ^{13}C{^{1}H} NMR (126 MHz, CDCl$_3$) δ 10.6, 30.6, 56.3, 56.3, 56.9, 71.6, 97.6, 111.2, 124.3, 143.2, 148.7, 150.8; HMRS (NSI-FTMS) *m/z*: [M+Na]$^+$ calcd for [C$_{12}$H$_{18}$O$_4$Na] 249.1097; Found 249.1092.

1-(2,4,5-Trimethoxyphenyl)propan-1-one 25 [73]

1-(2,4,5-Trimethoxyphenyl)propan-1-ol **24** (1.0001 g, 4.42 mmol) was dissolved in dichloromethane (5 mL), and MnO$_2$ (3.84 g, 44.2 mmol, 10 equiv.) added in one portion. The suspension was heated using a heating mantle under reflux for 24 hr. After cooling, the reaction mixture was filtered through a pad of celite, and the solvents were removed under reduced pressure. The residue was purified by column chromatography on silica gel (eluent: hexanes/ethyl acetate 5:1) to provide 1-(2,4,5-trimethoxyphenyl)propan-1-one as a colourless solid (0.4596 g, 46%); mp 105 – 107 °C [lit.[74]

107 – 108 °C]; v_{max}(CH$_2$Cl$_2$)/cm^{-1} 2972, 2939, 2916, 2835, 1605, 1472, 1270, 1025; ^{1}H NMR (400 MHz, CDCl$_3$) δ 1.15 (t, J = 7.2 Hz, 3H), 2.97 (q, J = 7.2 Hz, 2H), 3.86 (s, 3H), 3.90 (s, 3H), 3.93 (s, 3H), 6.49 (s, 1H), 7.42 (s, 1H); ^{13}C{^{1}H} NMR (101 MHz, CDCl$_3$) δ 8.7, 37.2, 56.2, 56.3, 56.4, 96.6, 112.8, 119.2, 143.1, 153.6, 155.2, 200.8; HRMS (NSI-FTMS) m/z: [M+Na]$^+$ calcd for [C$_{12}$H$_{16}$O$_4$Na] 247.0941; Found 247.0943.

(Z)-1-(2,4,5-Trimethoxyphenyl)prop-1-en-1-yl acetate 26

A solution of n-BuLi in n-hexane (1.5 mL, 2.5 M, 3.75 mmol, 1.4 equiv) was added dropwise to a solution of diisipropylamine (0.62 mL, 4.42 mmol, 1.7 equiv) in anhydrous tetrahydrofuran (16 mL) at −78 °C. After 30 minutes, a solution of 1-(2,4,5-trimethoxyphenyl)propan-1-one **25** (0.5916 g, 2.6 mmol) in anhydrous tetrahydrofuran (16 mL) was added dropwise. After 45 minutes, acetic anhydride (0.52 mL, 5.5 mmol, 2.1 equiv.) was added dropwise, and the reaction mixture stirred for 44 hours at room temperature. Saturated aqueous NaHCO$_3$ (75 mL) and diethyl ether (10 mL) were added. The aqueous phase was extracted with Et$_2$O (2 x 75 mL), and the combined organic phases were washed with brine (75 mL), dried (Na$_2$SO$_4$), and concentrated under reduced pressure. The residue was recrystallized twice from isopropanol, and the mother liquors recrystallized. The resulting solids were re-dissolved in ether (30 mL), washed with aqueous HCl (1M, 15 mL x 2) dried with sodium sulphate, filtered, and the solvents removed under reduced pressure to provide (Z)-1-(2,4,5-trimethoxyphenyl)prop-1-en-1-yl acetate as a pale-yellow waxy solid (0.3571 g, 51%); v_{max} (CH$_2$Cl$_2$)/cm^{-1} 2937, 2847, 1752, 1610, 1509; ^{1}H NMR (400 MHz, CDCl$_3$) δ 6.84 (s, 1H), 6.51 (s, 1H), 5.80 (q, J = 7.0 Hz, 1H), 3.88 (s, 3H), 3.83 (s, 3H), 3.83 (s, 3H), 2.22 (s, 3H), 1.70 (d, J = 7.0 Hz, 3H); ^{13}C{^{1}H} NMR (101 MHz, CDCl$_3$) δ 168.7, 151.5, 149.7, 144.3, 143.0, 116.7, 115.6, 112.7, 98.3, 56.8, 56.7, 56.2, 20.8, 11.8; HRMS (NSI-FTMS) m/z: [M+H]$^+$ calcd for [C$_{14}$H$_{19}$O$_5$] 267.1227; Found 267.1227.

1-Oxo-1-(2,4,5-trimethoxyphenyl)propan-2-yl acetate 27

Racemic oxidation

NaHCO$_3$ (0.315 g, 3.75 mmol, 3 equiv.) and meta-chloroperoxybenzoic acid (77% w/w; 0.315 g) were added to dichloromethane (6.5 ml), and the mixture cooled to 0 °C. (Z)-1-(2,4,5-trimethoxyphenyl)prop-1-en-1-yl acetate **26** (0.325 g, 1.219 mmol) was added. The mixture was stirred for 16 h at room temperature, diethyl ether (10 mL) added, and the mixture washed with water (10 mL), aqueous Na$_2$CO$_3$ (3 x 10 mL), and brine (10 mL). The organic phase was dried over anhydrous MgSO$_4$, and the solvents removed under reduced pressure. The residue was purified using column chromatography on silica gel (eluent: hexanes/ethyl acetate 3:1) to give 1-oxo-1-(2,4,5-trimethoxyphenyl)propan-2-yl acetate as a colourless solid (0.177 g, 29% over two steps); mp 102 – 104 °C; v_{max} (CH$_2$Cl$_2$)/cm^{-1} 2939, 2850, 1740, 1605, 1515, 1469, 1404, 1223; ^{1}H NMR (500 MHz,

CDCl$_3$) δ 1.45 (d, J = 6.9 Hz, 3H), 2.14 (s, 3H), 3.87 (s, 3H), 3.93 (s, 3H), 3.96 (s, 3H), 6.00 (q, J = 6.9 Hz, 1H), 6.49 (s, 1H), 7.46 (s, 1H); ^{13}C{^{1}H} NMR (126 MHz, CDCl$_3$) δ 16.5, 21.0, 56.3, 56.4, 56.4, 75.2, 96.3, 113.2, 116.3, 143.6, 154.8, 155.3, 170.8, 195.7; HRMS (NSI-FTMS): m/z [M+Na]$^+$ Calcd for [C$_{14}$H$_{18}$O$_6$Na] 305.0996; Found 305.0988; HPLC (Daicel Chiralpak AD-H) (80:20, hexane:isopropanol, flow rate: 0.8 mL/min); 12.27 min (49.15%), 15.70 min (50.85%).

Asymmetric oxidation

A. Prepared according to the general procedure for TPPP enol ether/ester epoxidation, using catalyst **2** (0.0289 g, 0.041 mmol, 0.1 equiv.), the enol acetate (0.109 g, 0.410 mmol) and TPPP (0.371 g, 0.820 mmol, 2 equiv.) in chloroform (2.2 ml). The reaction was stirred for 72 hours at -45 °C. Purification by column chromatography on silica gel (eluent: hexanes/ethyl acetate 3:1) afforded 1-oxo-1-(2,4,5-trimethoxyphenyl)propan-2-yl acetate as a colourless gum (0.012 g, 6% over 2 steps); HPLC (Daicel Chiralpak AD-H) (80:20, hexane:isopropanol, flow rate: 0.8 mL/min); 12.23 min (24.76%), 15.63 min (75.24%).

B. Prepared according to the general procedure for TPPP enol epoxidation, using catalyst **2** (0.0224 g, 0.031 mmol, 0.11 equiv.), the repurified enol acetate (0.0763 g, 0.286 mmol) and TPPP (0.264 g, 0.58 mmol, 2 equiv.) in chloroform (1.5 ml). The reaction was stirred for 20 hours at –40 °C, and the solvents removed under reduced pressure. Purification by column chromatography on silica gel (eluent: hexanes/ethyl acetate 3:1) afforded 1-oxo-1-(2,4,5-trimethoxyphenyl)propan-2-yl acetate as a colourless gum (0.0258 g, 32%); HPLC (Daicel Chiralpak AD-H) (80:20, hexane:isopropanol, flow rate: 0.8 mL/min); 11.98 min (31.41%), 15.30 min (68.59%). [α]$_D^{26}$ = –21.7 (c = 0.6, CHCl$_3$).

Tatarinoid A 22 [42]

Racemic synthesis

Prepared according to the general procedure for protecting group removal using 1-oxo-1-(2,4,5-trimethoxyphenyl)propan-2-yl acetate **27** (0.139 g, 5 g, 0.492 mmol) and camphorsulfonic acid (0.125 g, 0.538 mmol, 1.1 equiv.) in methanol (7 ml). Purification by column chromatography on silica gel (eluent: hexanes/ethyl acetate 3:2) afforded (±)-tatarinoid A as a colourless gum (0.0876 g, 74%). v_{max} (CH$_2$Cl$_2$)/cm^{-1} 3463, 2936, 2847, 1648, 1603, 1515, 1467, 1271, 1221, 1114, 1025; ^{1}H NMR (500 MHz, CDCl$_3$) δ 1.35 (d, J = 6.8 Hz, 3H), 3.89 (s, 3H), 3.93 (s, 3H), 3.97 (s, 3H), 5.14 (q, J = 6.8 Hz, 1H), 6.49 (s, 1H), 7.48 (s, 1H); ^{13}C{^{1}H} NMR (126 MHz, CDCl$_3$) δ 21.3, 56.2, 56.3, 56.5, 72.9, 96.3, 113.1, 115.1, 143.6, 155.1, 155.6, 201.6; HPLC (Daicel Chiralcel OJ) (70:30, hexane:isopropanol, flow rate: 0.8 mL/min); 27.67 min (49.52%), 29.20 min (50.48%).

Asymmetric Synthesis

Prepared according to the general procedure for protecting group removal using 1-oxo-1-(2,4,5-trimethoxyphenyl)propan-2-yl acetate (0.053 g, 0.492 mmol) and camphorsulfonic acid (0.125 g, 0.538 mmol, 1.1 equiv.) in methanol (2.7 ml). Purification by column chromatography on silica gel

(eluent: hexanes/ethyl acetate 3:2) afforded (*R*)-(–)-tatarinoid A as a colourless gum (0.0282 g, 63%); $[\alpha]_D^{22}$ = –132.7 (c 0.22 in $CHCl_3$); HRMS (ASAP-TOF): *m/z* [M+H]$^+$ Calcd for $C_{12}H_{17}O_5$ 241.1076; Found 241.1073. HPLC (Daicel Chiralcel OJ) (70:30, hexane:isopropanol, flow rate: 0.8 mL/min); 26.73 min (73.99%), 28.41 min (26.01%).

DFT calculations

Density functional Theory (DFT) calculations were performed on the UEA 'Grace' and 'hpc' high performance computational clusters running Gaussian09 v.B01[75] employing 12 processors (Grace) or 16 processors (hpc) at a single dedicate node, using the B3LYP functional and the 6-31G(d) (6-31g*) basis set. The absence of imaginary (negative) vibrational frequencies determined by frequency calculations using the atomic coordinates of the optimised geometries confirmed that in each case true energy minima had been identified. Each transition state was confirmed by the presence of a negative vibrational frequency, with the reaction coordinate corresponding to the concerted lengthening of the N-O bond upon the approach of the alkene. The reaction paths were confirmed by computing points along each reaction pathway by determining the intrinsic reaction coordinates (IRCs) in both directions. Individual distances and angles were measured using Molden, and graphics and atom coordinate tables (for the SI) were generated using GaussView5 (Grace) and 5.7 (hpc).

Supporting information

Proton and carbon NMR spectra, HPLC traces, and results of DFT calculations are available in supporting information.

Acknowledgements

References

1- For example: (a) Davis, F. A. Recent applications of N-sulfonyloxaziridines (Davis oxaziridines) in organic synthesis. *Tetrahedron* **2018**, *74*, 3198; (b) Wang, H.; Andemichael,

Y. W.; Vogt F. G. A Scalable Synthesis of 2S-Hydroxymutilin via a Modified Rubottom Oxidation. *J. Org. Chem.,* **2009**, *74*, 478; (c) Nicolaou, K. C.; Lim, Y. H.; Becker J. Total Synthesis and Absolute Configuration of the Bisanthraquinone Antibiotic BE-43472B. *Angew. Chem. Int. Ed.,* **2009**, *48*, 3444; (d) White, J. D.; Demnitz, F. W. J.; Xu, Q.; Martin, W. H. C. Synthesis of an Advanced Intermediate for (+)-Pillaromycinone. Staunton−Weinreb Annulation Revisited. *Org. Lett.* **2008**, *10*, 2833; (e) Ley, S. V.; Sheppard, T. D.; Myers, R. M.; Chorghade, M. S. Chiral Glycolate Equivalents for the Asymmetric Synthesis of α-Hydroxycarbonyl Compounds. *Bull. Chem. Soc. Japan.,* **2007**, *80*, 1451; (f) Armstrong, A.; Gethin, D. M.; Wheelhouse, C. J. Furanose Synthesis via Regioselective Dihydroxylation of 1-Silyloxy-1,3-dienes: Application to the Furanose Unit of 4-epi-Hygromycin A. *Synlett*, **2004**, 350; (g) Roush, W. R.; Michaelides, M. R.; Tai, D. F.; Lesur, B. M;. Chong, W. K. M.; Harris, D. J. A highly stereoselective synthesis of (+)-olivin, the aglycon of olivomycin A. *J. Am. Chem. Soc.,* **1989**, *111*, 2984; (h) Semmelhack, M. F.; Appapillai, Y.; Sato, T. Stereospecific synthesis of the bicyclo[2.2.2] portion of granaticin; synthesis of sarubicin A. *J. Am. Chem. Soc.,* **1985**, *107*, 4577; (i) Kornfeld, E. C.; Fornefeld, E. J.; Kline, G. B.; Mann, M. J.; Morrison, D. E.; Jones, R. G.; Woodward, R. B. The Total Synthesis of Lysergic Acid. *J. Am. Chem. Soc.,* **1956**, *78*, 3087.

2-   Rubottom, G. M.; Vazquez, M. A.; Pelegrina, D. R. Peracid oxidation of trimethylsilyl enol ethers: A facile α-hydroxylation procedure. *Tetrahedron Lett.,* **1974**, *15*, 4319.

3-   Brook, A. G.; Macrae, D. M. 1,4-Silyl rearrangements of siloxyalkenes to siloxyketones during peroxidation. *J. Organomet. Chem.,* **1974**, *77*, C19.

4-   Hassner, A.; Reuss, R. H.; Pinnick, H. W. Synthetic methods. VIII. Hydroxylation of carbonyl compounds via silyl enol ethers. *J. Org. Chem.,* **1975**, *40*, 3427.

5-   Rubottom, G. M.; Marrero, R. Reaction of ketene bis(trimethylsilyl) acetals with m-chloroperbenzoic acid. Synthesis of α-hydroxycarboxylic acids. *J. Org. Chem.,* **1975**, *40*, 3783.

6-   (a) Davis, F. A.; Sheppard, A. C. Oxidation of silyl enol ethers using 2-sulfonyloxaziridines. Synthesis of α-siloxy epoxides and α-hydroxy carbonyl compounds. *J. Org. Chem.,* **1987**, *52*, 954; (b) Susanto, W.; Lam, Y. Oxidation reactions using polymer-supported 2-benzenesulfonyl-3-(4-nitrophenyl)oxaziridine. *Tetrahedron*, **2011**, *67*, 8353.

7-   McCormick, J. P.; Tomasik, W.; Johnson, M. W. α-Hydroxylation of ketones: Osmium tetroxide/N-methylmorpholine-N-oxide oxidation of silyl enol ethers. *Tetrahedron Lett.,* **1981**, *22*, 607.

8-   (a) Merrit, E. A.; Olofsson, B. α-Functionalization of Carbonyl Compounds Using Hypervalent Iodine Reagents. *Synthesis*, **2011**, 517; (b) Ochiai, M.; Miyamoto, K.; Yokota, Y.; Suefuji, T.; Shiro, M. Synthesis, Characterization, and Reaction of Crown Ether Complexes of Aqua(hydroxy)(aryl)iodonium Ions. *Angew. Chem. Int. Ed.,* **2005**, *44*, 75; (c) Moriarty, R. M.; Epa, W. R.; Penmasta, R.; Awasthi, A. K. Hypervalent iodine oxidation of trimethylsilyl enol ethers of

ketones: A direct synthesis of α-keto triflates. *Tetrahedron Lett.*, **1989**, *30*, 667; (d) Moriarty, R. M.; John, L. S.; Du, P. C. Hypervalent iodine in organic synthesis. A novel route to the dihydroxyacetone side-chain in the pregnene series. *J. Chem. Soc., Chem. Comm.,* **1981**, 641.

9-   Li, H.-J.; Zhao, J.-L.; Chen, Y.-J.; Liu, L.; Wang, D.; Li, C.-J. Water-promoted direct aerobic oxidation of enol silyl ether to α-hydroxyl ketones without catalyst. *Green Chem.*, **2005**, *7*, 61.

10-   Arai, T.; Sato, T.; Kanoh, H.; Kaneko, K.; Oguma, K.; Yanagisawa, A. Organic–Inorganic Hybrid Polymer-Encapsulated Magnetic Nanobead Catalysts. *Chem. Eur. J.,* **2008**, *14*, 882.

11-   (a) Gardner, P. D. Organic Peracid Oxidation of Some Enol Esters Involving Rearrangement. *J. Am. Chem. Soc.,* **1956**, *78*, 3421; (b) Shine, H. J.; Hunt, G. E. The Epoxidation of 1-Acetoxycyclohexene and the Rearrangement of 1-Acetoxy-1,2-epoxycyclohexane. *J. Am. Chem. Soc.,* **1958**, *80*, 2434.

12-   Troisi, L.; Cassidei, L.; Lopez, L.; Mello, R.; Curci, R. Oxidations by methyl trifluoromethyl dioxirane. Epoxidation of enol ethers. *Tetrahedron Lett.,* **1989**, *30*, 257.

13-   (a) Wong, O. A.; Shi, Y. Organocatalytic Oxidation. Asymmetric Epoxidation of Olefins Catalyzed by Chiral Ketones and Iminium Salts. *Chem. Rev.,* **2008**, *108*, 3958; (b) Katsuki, T. Nb(salen)-Catalyzed Sulfoxidation. *Synlett*, **2003**, 281.

14-   Maekawa, H.; Itoh, K.; Goda, S.; Nishiguchi, I. Enantioselective electrochemical oxidation of enol acetates using a chiral supporting electrolyte. *Chirality*, **2003**, *15*, 95.

15-   Davis, F. A.; Chen, B.-C. Asymmetric hydroxylation of enolates with N-sulfonyloxaziridines. *Chem Rev.*, **1992**, *92*, 919.

16-   Patonay, T.; Jekő, J.; Kiss-Szikszai, A.; Lévai, A. Synthesis of Racemic and Enantiomerically Enriched a-Oxyfunctionalized Benzocyclanones and Chromanones by Dimethyldioxirane and Dimethyldioxirane/Mn(III) salen System. *Monatsh. Chem.,* **2004**, *135*, 743.

17-   Reddy, D. R.; Thornton, E. R. A very mild, catalytic and versatile procedure for α-oxidation of ketone silyl enol ethers using (salen)manganese(III) complexes; a new, chiral complex giving asymmetric induction. A possible model for selective biochemical oxidative reactions through enol formation. *J. Chem. Soc., Chem. Commun.,* **1992**, 172.

18-   (a) Adam, W.; Fell, R. T.; Mock-Knoblauch, C.; Saha-Möller, C. R. Synthesis of optically active α-hydroxycarbonyl compounds by (salen)Mn(III)-catalyzed oxidation of silyl enol ethers and silyl ketene acetals. *Tetrahedron Lett,*. **1996**, *37*, 6531; (b) Adam, W.; Fell, R. T.; Stegmann, V. R.; Saha-Möller, C. R. Synthesis of Optically Active α-Hydroxy Carbonyl Compounds by the Catalytic, Enantioselective Oxidation of Silyl Enol Ethers and Ketene Acetals with (Salen)manganese(III) Complexes. *J. Am. Chem. Soc.,* **1998**, *120*, 708.

19-   Fukuda, T.; Katsuki, T. Mn-salen catalyzed asymmetric oxidation of enol derivatives. *Tetrahedron Lett.,* **1996**, *37*, 4389.

20-   Koprowski, M.; Luczak, J.; Krawczyk, E. Asymmetric oxidation of enol phosphates to α-

hydroxy ketones by (salen)manganese(III) complex. Effects of the substitution pattern of enol phosphates on the stereochemistry of oxygen transfer. *Tetrahedron*, **2006**, *62*, 12363.

21- Morikawa, K.; Park, J.; Andersson, P. G.; Hashiyama, T.; Sharpless, K. B. Catalytic asymmetric dihydroxylation of tetrasubstituted olefins. *J. Am. Chem. Soc.,* **1993**, *115*, 8463.

22- Curran, D. P.; Ko, S.-B. Synthesis of Optically Active .alpha.-Hydroxy Lactones by Sharpless Asymmetric Dihydroxylations of Ketene Acetals, Enol Ethers, and Ene Lactones. *J. Org. Chem.,* **1994**, *59*, 6139.

23- Momiyama, N.; Yamamoto, H. Catalytic Enantioselective Synthesis of α-Aminooxy and α-Hydroxy Ketone Using Nitrosobenzene. *J. Am. Chem. Soc.,* **2003**, *125*, 6038.

24- Kawasaki, M.; Li, P.; Yamamoto, H. Enantioselective O-Nitroso Aldol Reaction of Silyl Enol Ethers. *Angew. Chem. Int. Ed.,* **2008**, *47*, 3795.

25- Butler, B.; Schultz, T; Simpkins, N. S. Chiral base mediated transformation of cyclic 1,3-diketones. *Chem. Commun.*, **2006**, 3634.

26- Adam, W.; Fell, R. T.; Saha-Möller, C. R.; Zhao, C.-G. Synthesis of optically active α-hydroxy ketones by enantioselective oxidation of silyl enol ethers with a fructose-derived dioxirane. *Tetrahedron: Asymmetry*, **1998**, *9*, 397.

27- Zhu, Y.; Tu, Y.; Yu, H.; Shi, Y. Highly enantioselective epoxidation of enol silyl ethers and esters. *Tetrahedron Lett.,* **1998**, *39*, 7819.

28- Solladié-Cavallo, A.; Lupattelli, P.; Jierry, L.; Bovicelli, P.; Angeli, F.; Antonioletti, R.; Klein, A. Asymmetric oxidation of silyl enol ethers using chiral dioxiranes derived from α-fluoro cyclohexanones. *Tetrahedron Lett.,* **2003**, *44*, 6523.

29- Lim, S. M.; Hill, N.; Myers, A. G. A Method for the Preparation of Differentiatedtrans-1,2-Diol Derivatives with Enantio- and Diastereocontrol. *J. Am. Chem. Soc.,* **2009**, *131,* 5763.

30- (a) Bulman Page, P. C.; Buckley, B. R.; Rassias, G. A.; Blacker, A. J. New Chiral Iminium Salt Catalysts for Asymmetric Epoxidation. *Eur. J. Org. Chem.,* **2006**, 803; (b) Bulman Page, P. C.; Bartlett, C. J.; Chan, Y.; Allin, S. M.; McKenzie, M. J. Lacour, J.; Jones, G. A. New biphenyl iminium salt catalysts for highly enantioselective asymmetric epoxidation: role of additional substitution and dihedral angle. *Org. Biomol. Chem.*, **2016**, *14*, 4220, and references therein; (c) Day, D. P.; Sellars, P. B. Recent Advances in Iminium-Salt-Catalysed Asymmetric Epoxidation. *Eur. J. Org. Chem.*, **2017**, 1034.

31- Campestrini, S.; Di Furia, F.; Labat, G.; Novello, F. Oxygen transfer from Ph_4PHSO_5 to manganese porphyrins: kinetics and mechanism of the formation of the oxo species in homogeneous solution. *J. Chem. Soc. Perkin Trans. 2,* **1994**, *10*, 2175.

32- (a) Bulman Page, P. C.; Appleby, L. F.; Chan, Y.; Day, D. P.; Buckley, B. R.; Slawin, A. M. Z.; Allin, S. M.; McKenzie, M. J. Kinetic Resolution in Asymmetric Epoxidation using Iminium Salt Catalysis. *J. Org. Chem.*, **2013**, *78*, 8074; (b) Bulman Page, P. C.; Chan, Y.; Day, D. P.

Enantioselective Epoxidation of Dihydroquinolines by Using Iminium Salt Organocatalysts. *Eur. J. Org. Chem*., **2014**, 8029, and references therein.

33- Bulman Page, P. C.; Buckley, B. R.; Heaney, H.; Blacker, A. J. Asymmetric Epoxidation of cis-Alkenes Mediated by Iminium Salts: Highly Enantioselective Synthesis of Levcromakalim. *Org. Lett.*, **2005**, *7*, 375.

34- Bulman Page, P. C.; Appleby, L. F.; Day, D. P.; Chan, Y.; Buckley, B. R.; Allin, S. M.; McKenzie, M. J. Highly Enantioselective Total Synthesis of (−)-(3′S)-Lomatin and (+)-(3′S,4′R)-trans-Khellactone. *Org. Lett.*, **2009**, *11*, 1991.

35- Bartlett, C. J.; Day, D. P.; Chan, Y.; Allin, S. M.; McKenzie, M. J.; Slawin, A. M. Z.; Bulman Page, P. C. Enantioselective Total Synthesis of (+)-Scuteflorin A Using Organocatalytic Asymmetric Epoxidation. *J. Org. Chem.,* **2012**, *77*, 772.

36- Bulman Page, P. C.; Chan, Y.; Abu Hassan Noor Armylisas; Alahmdi, M. Asymmetric Epoxidation of Chromenes Mediated by Iminium Salts: Synthesis of Mollugin and (3*S*,4*R*)-*trans*-3,4-Dihydroxy-3,4-Dihydromollugin. *Tetrahedron* **2016**, *72*, 8406.

37- (a) Bulman Page, P. C.; Parker, P.; Rassias, G. A.; Buckley, B. R.; Bethell, D. Iminium Salt-Catalysed Asymmetric Epoxidation using Hydrogen Peroxide as Stoichiometric Oxidant. *Adv. Synth. Catal*., **2008**, *350*, 1867; (b) Bulman Page, P. C.; Parker, P.; Buckley, B. R.; Rassias, G. A.; Bethell, D. Organocatalysis of asymmetric epoxidation by iminium salts using sodium hypochlorite as the stoichiometric oxidant. *Tetrahedron,* **2009**, *65*, 2910.

38- Buckley, B. R.; Chan, Y.; Dreyfus, N.; Elliott, C. E.; Marken, F.; Bulman Page, P. C. Harnessing applied potential to oxidation in water. *Green Chem*., **2012**, *14*, 2221, and references therein.

39- Yu, J.-Q.; Wu, H.-C.; Corey, E. J. Pd(OH)$_2$/C-Mediated Selective Oxidation of Silyl Enol Ethers by tert-Butylhydroperoxide, a Useful Method for the Conversion of Ketones to α,β-Enones or β-Silyloxy-α,β-enones. *Org. Lett.,* **2005**, *7*, 1415.

40- Hayashi, T.; Fujiwa, T.; Okamoto, Y.; Katsuro, Y.; Kumada, M. Cross-Coupling of Enol Phosphates with Trimethylsilylmethylmagnesium Halides Catalyzed by Nickel or Palladium Complexes; A Selective Synthesis of Allylsilanes. *Synthesis*, **1981**, 1001.

41- Noji, M.; Ohno, T.; Fuji, K.; Futaba, N.; Tajima, H.; Ishii, K. Secondary Benzylation Using Benzyl Alcohols Catalyzed by Lanthanoid, Scandium, and Hafnium Triflate. *J. Org. Chem.,* **2003**, *68*, 9340.

42- Tong, X.-G.; Wu, G.-S.; Huang, C.-G.; Lu, Q.; Wang, Y.-H.; Long, C.-L.; Luo, H.-R.; Zhu, H.-J.; Cheng Y.-X. Compounds from Acorus tatarinowii: Determination of Absolute Configuration by Quantum Computations and cAMP Regulation Activity. *J. Nat. Prod*. **2010**, *73*, 1160.

43- Slutskyy, Y.; Jewell, W. T.; Lucero, C. G. Syntheses of (−)-Tatarinoid A, (±)-Tatarinoid B, and (−)-Tatarinoid C. *Tetrahedron Lett.* **2013**, *54*, 210.

44-   Okada, H.; Mori, T.; Saikawa, Y.; Nakata, M. Formation of α-hydroxyketones via irregular Wittig reaction. *Tetrahedron Lett.* **2009**, *50*, 1276.

45-   (a) Becke, A. D. Density-functional thermochemistry. III. The role of exact exchange. *J. Chem. Phys.* **1993**, *98*, 5648. (b) Lee, C.; Yang, W.; Parr, R. G. Development of the Colle-Salvetti correlation-energy formula into a functional of the electron density. *Phys. Rev. B* **1988**, *37*, 785. (c) Stephens, P. J.; Devlin, F. J.; Chabalowski, C. F.; Frisch, M. J. Ab Initio Calculation of Vibrational Absorption and Circular Dichroism Spectra Using Density Functional Force Fields. *J. Phys. Chem.* **1994**, 98, 11623.

46-   Ditchfield, R.; Hehre, W. J.; Pople, J. A. Self-Consistent Molecular-Orbital Methods. IX. An Extended Gaussian-Type Basis for Molecular-Orbital Studies of Organic Molecules. *J. Chem. Phys.* **1971**, *54*, 724.

47-   Bohr, L.; Lusinchi, M.; Lusinchi, X. Oxygen atom transfer from a chiral oxaziridinium salt. Asymmetric epoxidation of unfunctionalized olefins. *Tetrahedron* **1999**, *55*, 141.

48-   (a) Bach, R. D.; Owensby, A. L.; Gonzalez, C.; Shlegel, H. B.; McDovall, J. S. Transition structure for the epoxidation of alkenes with peroxy acids. A theoretical study. *J. Am. Chem. Soc.* **1991**, *113*, 2338. (b) Yamabe, S.; Kondou, C.; Minato, T. A Theoretical Study of the Epoxidation of Olefins by Peracids. *J. Org. Chem.* **1996**, *61*, 616. (c) Bach, R. D.; Andrós, J. L.; Owensby, A. L.; Shlegel, H. B.; McDovall, J. S. Electronic structure and reactivity of dioxirane and carbonyl oxide. *J. Am. Chem. Soc.* **1992**, *114*, 7207. (d) Manoharan, M.; Venuvanalingan, P. AM1 and PM3 transition structures for the epoxidation of alkenes and allene by methylated dioxiranes. *J. Mol. Struct. (Theochem)* **1997**, *394*, 41.

49-   Houk, K. N.; Liu, J.; DeMello, N. C.; Condroski, K. R. Transition States of Epoxidations: Diradical Character, Spiro Geometries, Transition State Flexibility, and the Origins of Stereoselectivity. *J. Am. Chem. Soc.* **1997**, *119*, 10147.

50-   Washington, I.; Houk, K. N. Transition States and Origins of Stereoselectivity of Epoxidations by Oxaziridinium Salts. *J. Am. Chem. Soc.* **2000**, *122*, 2948.

51-   (a) Fukui, K. Formulation of the reaction coordinate. *J. Phys. Chem.*, **1970**, *74*, 4161. (b) Fukui, K. The path of chemical reactions - the IRC approach. *Acc. Chem. Res.* **1981**, *14*, 363. (c) Maeda, S.; Harabuchi, Y.; Ono, Y.; Taketsugu, T.; Morokuma, K. Intrinsic reaction coordinate: Calculation, bifurcation, and automated search. *Int. J. Quantum Chem.* **2015**, *115*, 258.

52-   (a) Miertus, S.; Scrocco, E.; Tomasi, J. Electrostatic interaction of a solute with a continuum. A direct utilizaion of AB initio molecular potentials for the prevision of solvent effects. *Chem. Phys.* **1981**, *55*, 117. (b) Barone, V.; Cossi, M.; Tomasi, J. Geometry optimization of molecular structures in solution by the polarizable continuum model. *J. Comput. Chem.* **1998**, *19*, 404. (c) for a recent review, see: Lipparini, F.; Mennucci, B. Perspective: Polarizable continuum models for quantum-mechanical descriptions. *J. Chem. Phys.* **2016**, *144*, 160901/1.

53- Johnson, E. R.; Keinan, S.; Mori-Sánchez, P.; Contreras-García, J.; Cohen, A. J.; Yang, W. *J. Am. Chem. Soc.*, **2010**, *132*, 6498.

54- (a) Takahashi, O.; Kohno, Y.; Nishio, M. *Chem. Rev.* **2010**, *110*, 6049; (b) Tsuzuki, S. *Ann. Rep. Prog. Chem., Sect. C: Phys. Chem.*, **2012**, *108*, 69.

55- Carrilo, R.; López-Rodriguez, M.; Martín, V. S.; Martín, T. Quantification of a CH–π interaction responsible for chiral descrimination and evaluation of its contribution to enantioselectivity. *Angew. Chem. Int. Ed.* **2009**, *48*, 7803.

56- Maekawa, H.; Hoh, K.; Goda, S.; Nishiguchi, I. Enantioselective electrochemical oxidation of enol acetates using a chiral supporting electrolyte. *Chirality* **2003**, 15, 95.

57- Noji, M.; Ohno, T.; Fuji, K.; Futaba, N.; Tajima, H.; Ishii, K. Secondary Benzylation Using Benzyl Alcohols Catalyzed by Lanthanoid, Scandium, and Hafnium Triflate. *J. Org. Chem.* **2003**, *68*, 9340.

58- Jiang, H.; Cheng, Y.; Zhang, Y.; Yu, S. Sulfonation and Trifluoromethylation of Enol Acetates with Sulfonyl Chlorides Using Visible-Light Photoredox Catalysis. *Eur. J. Org. Chem.* **2013**, *24*, 5485.

59- Tang, Y.; Fan, Y.; Zhang, Y.; Li, X.; Xu, X. Metal-Free tert-Butyl Hydrogenperoxide (TBHP) Mediated Radical Alkylation of Enol Acetates with Alcohols: A New Route to β-Hydroxy Ketones. *Synlett* **2016**, *27*, 1860.

60- Tang, Y.; Fan, H.; Gao, X.; Li, X.; Xu, X. Synthesis of β-keto-sulfones via metal-free TBAI/TBHP mediated oxidative cross-coupling of vinyl acetates with sulfonylhydrazides. *Tetrahedron Lett.* **2015**, *56*, 5616.

61- (a) Schmidt, R. G.; Bayburt, E. K.; Latshaw, S. P.; Koenig, J. R.; Daanen, J. F.; McDonald, H. A.; Bianchi, B. R.; Zhong, C.; Joshi, S.; Honore, P.; Marsh, K. C.; Lee, C.-H.; Faltynek, C. R.; Gomtsyan, A. Chroman and tetrahydroquinoline ureas as potent TRPV1 antagonists. *Bioorg. Med. Chem. Lett.* **2011**, *21*, 1338; (b) Fang, Y.; Rogness, D. C.; Larock, R. C.; Shi, F. Formation of Acridones by Ethylene Extrusion in the Reaction of Arynes with β-Lactams and Dihydroquinolinones. *J. Org. Chem.* **2012**, *77*, 6262.

62- Zhu, M.; Kim, M. H.; Lee, S.; Bai, S. J.; Kim, S. H.; Park, S. B. Discovery of Novel Benzopyranyl Tetracycles that Act as Inhibitors of Osteoclastogenesis Induced by Receptor Activator of NF-κB Ligand. *J. Med. Chem.* **2010**, *53*, 8760.

63- Lim, S. M.; Hill, N.; Myers, A. G. A Method for the Preparation of Differentiatedtrans-1,2-Diol Derivatives with Enantio- and Diastereocontrol. *J. Am. Chem. Soc.* **2009**, *131*, 5763.

64- Langvik, O.; Mäki-Arvela, P.; Aho, A.; Saloranta, T.; Murzin, D. Yu; Leino, R. Regioselective Hydrogenation of 1,2-Indanedione Over Heterogeneous Pd and Pt Catalysts. *Catalysis Lett.* **2013**, *143*, 142.

65- Huang, X.; Liang, X.; Yuan, J.; Ni, Z.; Zhou, Y.; Pan, Y. Aerobic copper catalyzed α-

oxyacylation of ketones with carboxylic acids. *Org. Chem. Front.* **2017**, *4*, 163.

66- Kajiro, H.; Mitamura, S.; Mori, A.; Hiyama, T. Scandium trifluoromethanesulfonate-catalyzed mild, efficient, and selective cleavage of acetates bearing a coordinative group. *Tetrahedron Lett.* **1999**, *40*, 1689.

67- Baskaran, S.; Das, J.; Chandrasekaran, S. Heterogeneous permanganate oxidations: an improved procedure for the direct conversion of olefins to .alpha.-diketones/.alpha.-hydroxy ketones. *J. Org. Chem.* **1989**, *54*, 5182.

68- Krawczyk, E.; Mielniczak, G.; Owsianik, K.; Łuczak, J. Asymmetric oxidation of enol phosphates to α-hydroxy ketones using Sharpless reagents and a fructose derived dioxirane *Tetrahedron: Asymmetry* **2012**, *23*, 1480.

69- Cazetta, T.; Lunardi, I.; Conceição, G. J. A.; Moran, P. J. S.; Rodrigues, J. A. R. *Trichosporon cutaneum*-promoted deracemization of (±)-2-hydroxindan-1-one: A mechanistic study *Tetrahedron: Asymmetry* **2007**, *18*, 2030.

70- Bortolini, O.; Fantin, G.; Fogagnolo, M.; Giovannini, P. P.; Guerrini, A.; Medici, A. An Easy Approach to the Synthesis of Optically Active vic-Diols: A New Single-Enzyme System. *J. Org. Chem.* **1997**, *62*, 1854.

71- Yanagisawa, A.; Lin, Y.; Takeishi, A.; Yoshida, K. Enantioselective Nitroso Aldol Reaction Catalyzed by a Chiral Phosphine-Silver Complex. *Eur. J. Org. Chem.* **2016**, 5355.

72- Alesso, E.; Torviso, R.; Lantaño, B.; Erlich, M.; Finkielsztein, L. M.; Moltrasio, G.; Aguirre, J. M.; Brunet, E. Synthesis of 1-ethyl-2-methyl-3-arylindanes. Stereochemistry of five-membered ring formation. *Arkivoc* **2003**, 283.

73- Park, C. H.; Kim, K. H.; Lee, I. K.; Lee, S. Y.; Choi, S. U.; Lee, J. H.; Lee, K. R. Phenolic constituents of Acorus gramineus *Arch. Pharm. Res.* **2011**, *34*, 1289..

74- Högberg, T.; Bengtsson, S.; Johansson, L.; Ström, P.; de Paulis, T.; Hall, H.; Ögren, S. O. Potential antipsychotic agents. 5. Synthesis and antidopaminergic properties of substituted 5,6-dimethoxysalicylamides and related compounds. *J. Med. Chem.* **1990**, *33*, 1155.

75- Gaussian 09, Revision B.02, Frisch, M. J.; Trucks, G. W.; Schlegel, H. B.; Scuseria, G. E.; Robb, M. A.; Cheeseman, J. R.; Scalmani, G.; Barone, V.; Petersson, G. A.; Nakatsuji, H.; Li, X.; Caricato, M.; Marenich, A.; Bloino, J.; Janesko, B. G.; Gomperts, R.; Mennucci, B.; Hratchian, H. P.; Ortiz, J. V.; Izmaylov, A. F.; Sonnenberg, J. L.; Williams-Young, D.; Ding, F.; Lipparini, F.; Egidi, F.; Goings, J.; Peng, B.; Petrone, A.; Henderson, T.; Ranasinghe, D.; Zakrzewski, V. G.; Gao, J.; Rega, N.; Zheng, G.; Liang, W.; Hada, M.; Ehara, M.; Toyota, K.; Fukuda, R.; Hasegawa, J.; Ishida, M.; Nakajima, T.; Honda, Y.; Kitao, O.; Nakai, H.; Vreven, T.; Throssell, K.; Montgomery, Jr., J. A.; Peralta, J. E.; Ogliaro, F.; Bearpark, M.; Heyd, J. J.; Brothers, E.; Kudin, K. N.; Staroverov, V. N.; Keith, T.; Kobayashi, R.; Normand, J.; Raghavachari, K.; Rendell, A.; Burant, J. C.; Iyengar, S. S.; Tomasi, J.; Cossi, M.; Millam, J. M.; Klene, M.; Adamo, C.; Cammi, R.; Ochterski, J. W.;

Martin, R. L.; Morokuma, K.; Farkas, O.; Foresman, J. B.; Fox, D. J. Gaussian, Inc., Wallingford CT, 2016.